

SOUTHWEST RESEARCH INSTITUTE  
Post Office Drawer 28510, 6220 Culebra Road  
San Antonio, Texas 78228-0510

# A STUDY OF THE EROSIONAL/CORROSIONAL VELOCITY CRITERION FOR SIZING MULTIPHASE FLOW LINES

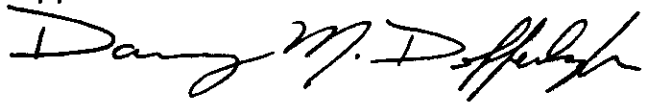
By  
Steven J. Svedeman

PHASE II FINAL REPORT  
SwRI Project 04-2433

Prepared For  
Minerals Management Service  
U.S. Department of the Interior  
Reston, Virginia

October 30, 1990

Approved:



---

Danny M. Deffenbaugh, Director  
Department of Fluid Systems

# TABLE OF CONTENTS

<u>Section</u>	<u>Page</u>
LIST OF FIGURES .....	iii
LIST OF TABLES .....	v
DISCLAIMER .....	vi
ACKNOWLEDGEMENTS .....	vii
EXECUTIVE SUMMARY .....	viii
1.0 INTRODUCTION .....	1
2.0 FIELD DATA SURVEY .....	3
2.1 Data Gathering .....	3
2.2 Summary of Field Data.....	3
2.2.1 Data Set 1.....	3
2.2.2 Data Set 2.....	17
3.0 ADDITIONAL EROSION/CORROSION DATA.....	28
3.1 Erosion/Corrosion Study of Solids Free Gas Wells.....	28
3.2 Erosion in Blow-Out Prevention Systems .....	28
3.3 Laboratory Study of Fitting Erosion.....	30
4.0 CONCLUSIONS .....	34
4.1 Clean Service.....	36
4.2 Erosion .....	36
4.3 Corrosion .....	41
4.4 Erosion and Corrosion .....	42
5.0 RECOMMENDATIONS AND FUTURE WORK .....	42
5.1 Recommendations .....	42
5.2 Future Work.....	44
REFERENCES .....	46

## LIST OF FIGURES

<u>Figure</u>		<u>Page</u>
2.1	Operating Velocity Compared with Erosional Velocity with $C = 100$ ..	8
2.2	Plot of Actual "Operating" C-value (calculated from operating data) and $CO_2$ Partial Pressure.....	9
2.3	Plot of Water Production versus $CO_2$ Partial Pressure.....	10
2.4	Plot of Water Production versus Operating Velocity.....	11
2.5	Plot of Water Production on an Expanded Scale versus Operating Velocity.....	12
2.6	Plot of Operating Temperature versus Velocity.....	13
2.7	Plot of Gas to Liquid Ratio versus Operating Velocity .....	14
2.8	Plot of Superficial Gas Velocity versus Superficial Liquid Velocity....	15
2.9	Flow Regime Boundary Map for Horizontal Pipe Showing Taitel and Dukler [5] and Mandhane et al [6] Boundaries .....	16
2.10	Plot of Wear Rate versus Operating Velocity .....	20
2.11	Plot of Erosional Velocity versus Actual Operating Velocity .....	21
2.12	Plot of Wear Rate versus Ratio of Actual Operating Velocity to Erosional Velocity.....	22
2.13	Plot of Wear Rate versus Water Production .....	23
2.14	Plot of Wear Rate versus Gas to Liquid Ratio.....	24
2.15	Plot of Wear Rate versus Gas Superficial Velocity .....	25
2.16	Plot of Wear Rate versus Liquid Superficial Velocity .....	26
2.17	Superficial Gas Velocity versus Superficial Liquid Velocity.....	27
3.1	Results of Corrosion Measurements by Duncan [7] .....	29
3.2	Specific Erosion Factors Given by Bourgoyne [8] .....	31
3.3	Wear Data on an Elbow Presented by Bourgoyne [8].....	32
3.4	Wear Rates for a $90^\circ$ Water Ell at Different Flow Velocities from Weiner and Tolle [9].....	33

## LIST OF FIGURES (cont'd)

<u>Figure</u>		<u>Page</u>
3.5	Wear Rate as a Function of Sand Flow Rate from Weiner and Tolle [9] .....	35
4.1	Comparison of Specific Wear Rates Reported by Bourgoyne [8] and Weiner and Tolle [9] for 90° Elbows with the Given Radius to Diameter Ratios ( $r/d$ ).....:	40

## LIST OF TABLES

<u>Table</u>		<u>Page</u>
2.1	Field Data Operating Conditions.....	5
2.2	Summary of Field Data Operating Conditions .....	18

## **DISCLAIMER**

The views and conclusions contained in this document are those of the author and should not be interpreted as necessarily representing the official policies or recommendations of the Department of Interior.

## ACKNOWLEDGEMENTS

The author wish to express their thanks to the members of the API Advisory Committee and especially Mr. David Miller and Mr. Mark Rubin from the Production Department of the American Petroleum Institute for coordinating this committee. Special thanks go to Mr. Charles Smith of Minerals Management Service, U.S. Department of Interior, for his thoughtful assistance in administering the program. The authors also extend their thanks to Mr. Ken Arnold of Paragon Engineering for identifying the critical need for this work and his valuable insight into the design and operation of offshore facilities. The API Advisory Committee members whose input was used to define the project direction include: Mr. John A. Herce of Exxon Production Research, Mr. Jim Higgason of Mobil Oil, Mr. Rick Resweber of Shell Offshore, Inc., Mr. R. Frank Robb of Arco Oil and Gas, and Mr. Dirk S. Swanson of Chevron USA.

## EXECUTIVE SUMMARY

The current recommended practice (API RP 14E) for sizing two-phase flow lines in offshore production piping is to limit the flow velocity to a value less than the fluid erosional velocity. A simple erosional velocity criterion based on a single empirical constant and the two-phase mixture density is provided as guidance to determine the velocity above which erosion may occur. This criterion is for clean service (non-corrosive and sand-free) and it is noted that the limits should be reduced if sand or corrosive conditions are present. However, no guidelines are provided for these corrections. It is widely accepted in the industry that this simple criterion is inadequate. The objective of this project is to upgrade this practice for more realistic conditions. This report presents the results of Phase II of this multiphase project. The initial phase reviewed the open literature and based on this review, a proposed format for an improved criteria was presented with specific details to be added in subsequent phases of this project.

Phase II of this project involved collecting and analyzing data obtained from API member companies. The data showed that pipe wear is a function of many different parameters and that one simple erosional velocity criterion (such as the present API RP 14E) cannot possibly predict wear in all cases. Depending upon the multiphase flow stream contents and operating parameters, different erosional velocity criterion will be required for the different wear mechanism. The primary wear categories that require different multiphase erosional velocity criterion are: "clean" service, erosion only (solids with no corrosion), corrosive multiphase service, and combined erosion and corrosion.



## 1.0 INTRODUCTION

There continues to be a significant amount of controversy regarding the API specification related to velocity limits [1] for horizontal two-phase flow lines for offshore production piping. This controversy will surely continue in the future due to the many variables involved in erosion and corrosion in production piping. Many investigators [2, 3, 4] have reviewed the velocity limits specified by API RP 14E and concluded that the limits are too conservative. The intention of this work is to review field data and determine if changes to the erosional velocity limits are appropriate. Any recommended changes need to provide a reasonable, safe, operating limit that does not cause excessive piping system operational or installation costs or excessive risk of failure.

Presently, the design guidelines recommend limiting the fluid velocity in two-phase flow lines to an erosional velocity ( $V_e$  (ft/sec)) defined by [1]:

$$V_e = \frac{C}{\sqrt{\rho}} \quad (\text{Eq. 1})$$

$C$  = 100 for continuous service,

= 125 for intermittent service

$\rho$  = mixture density (lbm/ft<sup>3</sup>)

The recommendations also require reducing the erosional velocity below the above calculated velocity if corrosion or solids (sand) are present. Guidelines on the amount of reduction to the calculated erosional velocity are not given.

The relatively simple calculation provides a good general velocity limit, but such a simple limit cannot possibly be applicable to the wide variety of conditions encountered in field operations. For this reason, the erosional velocity will be conservative in some applications and allow excessive wear in others. The intent of this work is, therefore, to develop some insight into where the limits should be adjusted upward or downward and what the important parameters are.

In the first phase of this project, the general oil and gas production literature was reviewed. One conclusion from this review was that no measurable erosive damage was documented for clean service. While there has been significant wear problems, all are accompanied by corrosive conditions and/or sand production. The primary location of these problems has been in fittings with elbows experiencing twice as much damage as tees, long radius bends, and straight runs downstream of chokes. To determine if there is a physical basis for these observations, we reviewed the fundamental erosion research literature.

The gas-liquid droplet erosion literature indicated that erosive wear due to droplet impact is proportional to the difference between the droplet velocity and a threshold velocity raised to a power. The significance of the threshold is that no erosive damage due to liquid impact occurs at velocities below the threshold. This threshold is about 400 feet per second. Since this is an order of magnitude above practical operating velocities, this confirms the assertion that no erosive damage has been experienced in the field for clean service.

The solid particle erosion literature indicates that solid particle erosion is proportional to the kinetic energy of individual particles. Erosive wear can occur at all velocities, so that for solid particle impacts a small acceptable wear rate is defined. With this wear limit, the kinetic energy models can be solved for velocity, so that an "erosional velocity" is proportional to the square root of the mass of the particles. However, this "erosional velocity" is based on the particle velocity. In order to develop a relationship for flow velocity, the literature on wear in pneumatic conveyor systems was reviewed.

The pneumatic conveyor literature identified elbows as the primary area of concern and presented models for wear rates in elbows as a function of density ratio of the solid particles to conveyor gas. The erosional velocity from these models is in the form of an empirical constant divided by a root of the density ratio. This root varied between 2 and 3 for practical velocities and particle loadings.

The erosion/corrosion literature indicates that in the absence of solid particles, wear rate increases with flow velocity. Corrosion in the presence of solid particle impacts follows the same general models as solid impact erosion, except that the target properties are those of the brittle corrosion products and not the base metal.

The conclusions from the Phase I work are:

- (1) No erosional velocity limit is required for non-corrosive sand-free service.
- (2) Erosional velocity ( $V_e$ ) for sand producing service is a function of an empirical constant (K) and the density ratio (Z) of sand density to gas density:

$$V_e = \frac{K}{\sqrt[n]{Z}} \quad (\text{Eq. 2})$$

- (3) The values of K and n are functions of corrosive conditions, fitting geometry and material properties of the fittings.

In this phase of the project, field data was requested from several companies with the intent of using this data to check the results of the Phase I work and to attempt to define the values of  $K$  and  $n$  in the erosional velocity equation for some fitting geometries and flow streams. The following section reviews the field data that was obtained and also reviews some other wear data from the open literature.

## **2.0 FIELD DATA SURVEY**

### **2.1 Data Gathering**

At the start of this project, many people indicated a willingness to provide erosion/corrosion data from their field operations. To start gathering data, API sent out a letter and a form requesting erosion/corrosion data to about 100 people on the API RP 14E committee. From these requests only two responses were received. Several phone calls were made to API member companies to solicit data with only limited success. Based on the phone conversations, it appears erosion/corrosion data exists at many companies but not in a form that is useful for determining the mechanism of pipe wear. The periodic inspection of piping is done and logged to monitor pipe wear, but the data on fluid flow is not recorded along with the wear data. The people contacted said it would take a substantial amount of time and effort to match the wear data with the production data and funds and manpower were not available to do this. This same theme was repeated by several companies.

The data sent in by one company was in a different form from the rest of the field data received in that it did not report wear rates, but indicated problems encountered. For this reason, the field data is broken into two groups for presentation in the next two sections.

### **2.2 Summary of Field Data**

#### **2.2.1 Data Set 1**

Operational data from two different gas fields was reported along with the piping problems encountered. Detailed data on measured wear rates in fittings was not available, but piping failures and the associated replacement items were reported. From this data, a general indication of whether the well was operating in an erosive or corrosive environment could be seen. The two fields had significantly different operating conditions. One field had relatively low flow rates and reported no piping problems over the 3 to 6 year reporting period. The other field operated at much higher flow rates and reported several piping failures due to erosion or corrosion.

The piping material for both fields was A-106-B with pipe diameters ranging from 1.5" to 6". Table 2.1 presents the well operating conditions and indicates if the piping experienced erosion or corrosion problems. The reported problems were either failures downstream of a choke, threadolet "washout," or valve wear problems. Figure 2.1 shows a plot of the actual operating velocity plotted against the erosional velocity (calculated from API RP 14E with  $C = 100$ ) with reported piping problems plotted as solid symbols. The points above the diagonal line indicate operation above the erosional velocity and these points generally have piping problems reported. In addition to the problem points above the diagonal line, there are several points below the line that experienced piping problems. Of the nine points significantly below the diagonal line, two points (the 2 with the lowest operating velocities) had much higher water production (on a BBL/MMSCF basis) than the other wells, and the other seven points had relatively high (0.2 to 1.0%) CO<sub>2</sub> content.

Figure 2.2 shows the same data plotted as CO<sub>2</sub> partial pressure versus the operating "C" value (the value of "C" was calculated from the erosional velocity equation based on actual operating velocity and mixture density). This plot clearly shows the trend of increasing frequency of problems with increasing "C" value or partial pressure (not all of the data points had a reported value of CO<sub>2</sub> so some of the data in Figure 2.1 is not shown in Figure 2.2). The one point showing no piping problems at a high CO<sub>2</sub> content was unique compared to the rest of the field in that its production pressure was 1650 psi versus about 1250 to 450 psi for the rest of the data. This point also was the smallest line size at 1.5" pipe compared to 3", 4", or 6" for the rest of the data points in the plot.

Figure 2.3 shows the CO<sub>2</sub> content plotted with the water production with the trend indicating little water needs to be present for CO<sub>2</sub> related piping problems to occur. Figures 2.4 and 2.5 both show water production plotted with operating velocity at different plotting scales. These plots again indicated that the pipe failures corresponded to higher velocity wells that produced relatively little water. The effect of temperature on the erosion and corrosion problem is shown in Figure 2.6. This plot shows that, as expected, the higher frequency of piping problems occur at elevated flow rates and temperatures. Figure 2.7 shows increased incidence of piping problems at higher gas/liquid ratio (liquid includes water and condensate) and higher operating velocities.

Figure 2.8 shows the data plotted as superficial gas velocity against superficial liquid velocity. This plotting format is used to determine the two-phase flow regime as mapped in Figure 2.9. The velocity data in Figure 2.8 are in the same units (m/sec) as Figure 2.9, so a direct comparison can be made. Figure 2.9 shows that above a superficial gas velocity of

Table 2.1 Field Data Operating Conditions

Pipe I.D. (in)	Pressure (psi)	Temperature (°F)	Gas Production (MSCFD)	Operating Velocity (ft/sec)	Erosional Velocity (ft/sec)	Operating C Value	Water Production (BBL/MMSCF)	Condensate Production (BBL/MMSCF)	Sand Production (y/n)	CO2 (%)	Gas/Liquid Ratio (CF/BBL)	Mixture Density (lbm/ft3)	Problems Reported (y/n)
3.62	1250	180	50000	103.49	55.51	186	1.5	2.5	n	1.7	250000	3.24	y
3.62	1250	180	44000	91.07	55.33	165	0.5	5	y	1.1	181818	3.27	y
3.62	1250	180	41000	84.86	55.62	153	1.2	2.2	n	2	294118	3.23	y
2.3	460	110	7304	90.64	89.1	102	1	1	n	0.2	500000	1.26	y
3.62	1250	180	36000	74.51	55.59	134	1.5	2	n		285714	3.24	y
5.5	1250	180	70000	62.77	55.05	114	0	7.5	y		133333	3.3	
2.3	460	110	5650	70.11	89.1	79	1	1	n	0.2	500000	1.26	y
3.62	1250	180	36600	75.76	55.87	115	0.1	2	n		476190	3.2	y
2.3	1200	140	12820	64.19	55.64	115	0.7	1.5		1	454545	3.23	y
3.62	1250	180	32500	67.27	53.88	125	2.5	12	y	1	68966	3.44	y
3.62	1250	180	35500	73.48	55.73	132	0	3	y	1.8	333333	3.22	y
2.3	460	110	7604	94.36	88.43	107	3	1	n	0.25	250000	1.28	n
2.3	1200	140	11426	57.21	55.34	103	0.3	3.9		0.5	238095	3.27	y
2.3	1200	140	12800	64.09	55.49	116	2	0.8	n	1	357143	3.25	y
2.3	1200	140	10059	50.37	55.54	91	0.9	1.9		1	357143	3.24	y
2.3	460	110	4650	57.7	89.1	65	1	1	n	0.2	500000	1.26	y
2.3	1200	140	8939	44.76	55.26	81	0.5	4.3		0.6	208333	3.28	n
2.3	460	110	5349	66.38	89.1	65	1	1	n	0.3	500000	1.26	n
2.3	1200	140	5000	25.04	55.61	45	0.3	2.2		1	400000	3.23	y
2.3	250	90	3100	68.3	81.38	84	145	0	n	0	6897	1.51	n
1.1	1650	90	1600	23.35	43.48	54	4	5	n	2.8	111111	5.29	n
2.3	250	90	4400	96.94	118.44	82	0.1	0.1	n	0	500000	0.71	n
2.3	1200	140	6044	30.26	55.72	54	0.8	0.89		1	591716	3.22	y
2.3	484	100	978	11.33	81.02	14	18.67	0	n	0.3	53562	1.52	n

**Table 2.1 Field Data Operating Conditions (cont'd)**

Pipe I.D. (in)	Pressure (psi)	Temperature (F)	Gas Production (MSCFD)	Operating Velocity (ft/sec)	Erosional Velocity (ft/sec)	Operating C Value	Water Production (BBL/MMSCF)	Condensate Production (BBL/MMSCF)	Sand Production (y/h)	CO <sub>2</sub> (%)	Gas/Liquid Ratio (CF/BBL)	Mixture Density (lbm/ft <sup>3</sup> )	Problems Reported (y/n)
2.3	460	110	4225	52.43	89.1	59	1	1	n	0.2	500000	1.26	n
3.62	450	180	8000	46	93.41	49	0	1	n	0.8	1000000	1.15	y
2.3	1200	140	3196	16	55.24	29	1.4	3.2	n	0.5	217391	3.28	y
3.62	1250	180	8500	17.59	56.06	31	0	1	n	1	1000000	3.18	y
2.3	476	100	1292	15.22	87.43	17	0	0	n	0.25	***	1.31	n
2.3	460	110	2140	26.56	89.7	30	0.1	0	n		10000000	1.24	n
2.3	750	90	580	4.26	23.37	18	1350	3.7	y	0	739	18.31	y
2.3	475	100	25	0.3	87.52	0	0	0	n	0.3	***	1.31	n
2.3	750	90	1000	7.34	47.03	10	152	0	y	0	6579	4.52	y
2.3	482	100	133	1.55	69.77	2	71.4	0	n	0.1	14006	2.05	n
1.5	600	57	5820	117.6	68.71	171	0.17	18.4	n		53850	2.12	n
3.15	100	96	2340	69.37	96.34	72	0	436	n		2294	1.08	n
3.15	120	152	1146	31.16	51	61	1400	80	n		676	3.84	n
3.15	100	83	1830	52.99	108.45	49	163	84	n		4049	0.85	n
3.15	120	130	1035	27.13	59.88	45	850	150	n		1000	2.79	n
5.2	1050	111	16870	17.97	40.85	44	121	26	n		6803	5.99	n
3.75	950	64	12740	26.47	60.4	44	0	0	n		***	2.74	n
3.15	100	99	1110	33.09	77.88	42	396	259	n		1527	1.65	n
5.2	1050	60	20000	19.41	51.48	38	0.5	29	n		33898	3.77	n
1.5	2200	107	1180	7.13	19.55	36	92	925	n		983	26.17	n
3.15	120	133	1160	30.57	87.42	35	305	90	n		12532	1.31	n
1.5	180	93	143	10.3	29.64	35	2867	321	n		314	11.39	n
3.15	120	127	600	15.65	46.87	33	157	2040	n		455	4.55	n

Table 2.1 Field Data Operating Conditions (cont'd)

Pipe I.D. (in)	Pressure (psi)	Temperature (F)	Gas Production (MSCFD)	Operating Velocity (ft/sec)	Erosional Velocity (ft/sec)	Operating C Value	Water Production (BBL/MMSCF)	Condensate Production (BBL/MMSCF)	Sand Production (y/n)	CO2 (%)	Gas/Liquid Ratio (CF/BBL)	Mixture Density (lbm/ft <sup>3</sup> )	Problems Reported (y/n)
3.15	1100	107	5094	14	47.18	30	0	69			14493	4.49	n
3.5	1050	59	5570	11.91	43.04	28	0	128			7813	5.4	n
3.15	350	107	1160	10.02	40.82	25	0	893			1120	6	n
1.5	180	78	148	10.37	42.7	24	50	1600	y		606	5.48	n
3.15	100	81	866	24.98	104.05	24	224	43			3745	0.92	n
3.75	500	110	2000	8.59	40.13	21	0	624			1603	6.21	n
3.15	100	78	1060	30.41	145.75	21	5	77			12195	0.47	n
3.75	500	90	2550	10.57	55.62	19	142	16	y		6329	3.23	n
1.5	180	70	62	4.28	26.32	16	3160	1240	y		227	14.44	n
3.75	950	66	4130	8.61	59	15	6.3	0			158730	2.87	n
3.15	120	139	148	3.94	29.45	13	4486	1007			182	11.53	n
3.15	1000	84	1560	4.53	34.4	13	0	351			2849	8.45	n
5.2	1050	120	2044	2.21	21.78	10	1122	20.5			875	21.07	n
3.15	1100	118	900	2.52	29.09	9	209	300			1965	11.81	n
3.15	100	78	324	9.29	134.03	7	83	22			9524	0.56	n
3.5	400	80	440	2.57	39.31	7	520	113			1580	6.47	n
3.75	950	74	1220	2.58	40.44	6	163	0	y		6135	6.12	n
3.5	400	80	423	2.47	38.69	6	548	111			1517	6.68	n
3.5	400	80	420	2.45	38.44	6	578	85	y		1508	6.77	n
5.2	1050	120	3087	3.34	57.21	6	0	8.4	y		119048	3.06	n
3.75	300	102	86	0.61	18	3	8140	12			123	30.86	n
3.75	400	70	367	1.83	90.6	2	8	0			125000	1.22	n
3.75	500	76	80	0.32	16.12	2	7100	538			131	38.5	n
3.75	950	69	152	0.32	60.69	1	0	0			**	2.72	n
3.75	300	84	12	0.08	105.98	0	0	0			**	0.89	n

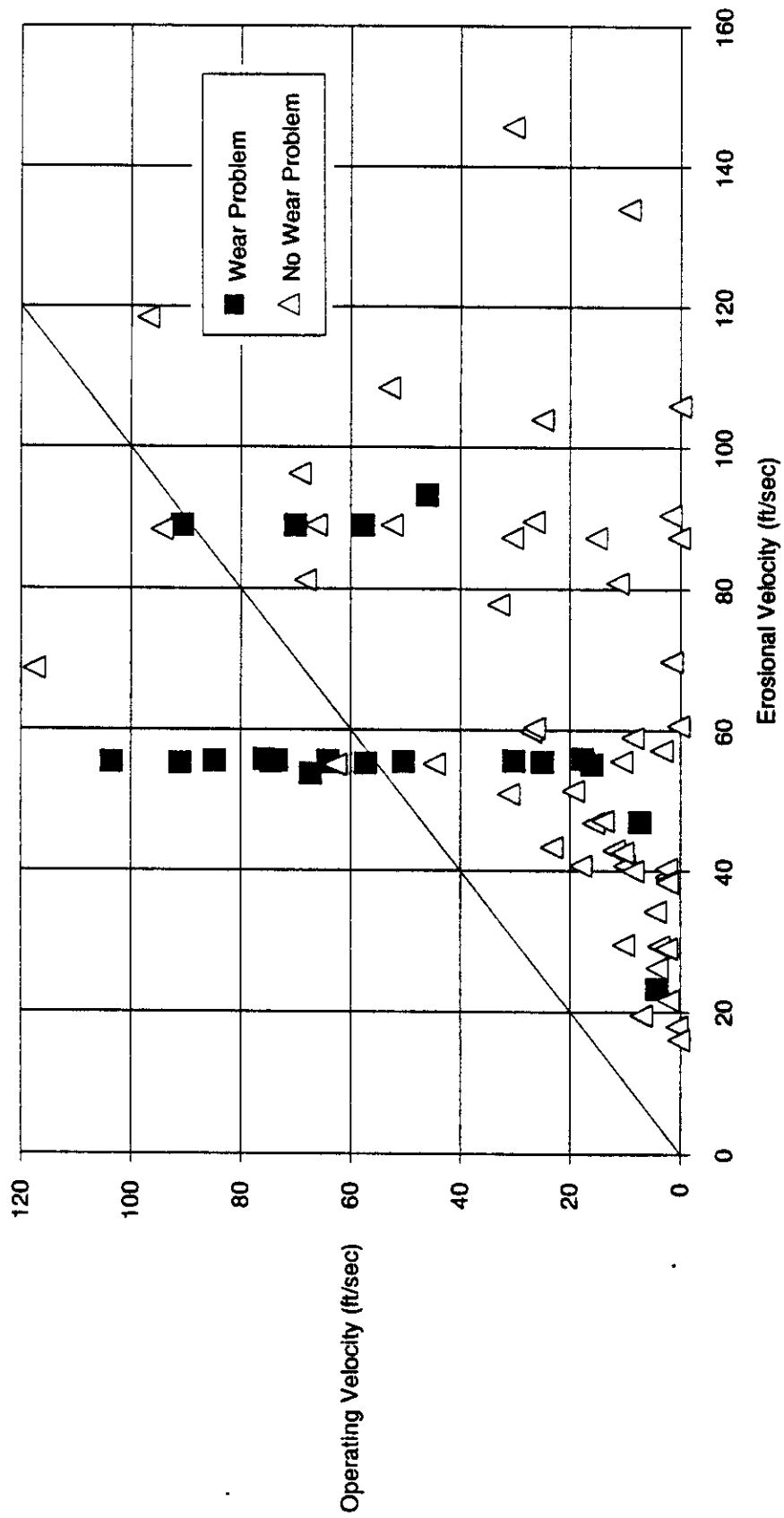


Figure 2.1 Operating Velocity Compared with Erosional Velocity with  $C = 100$



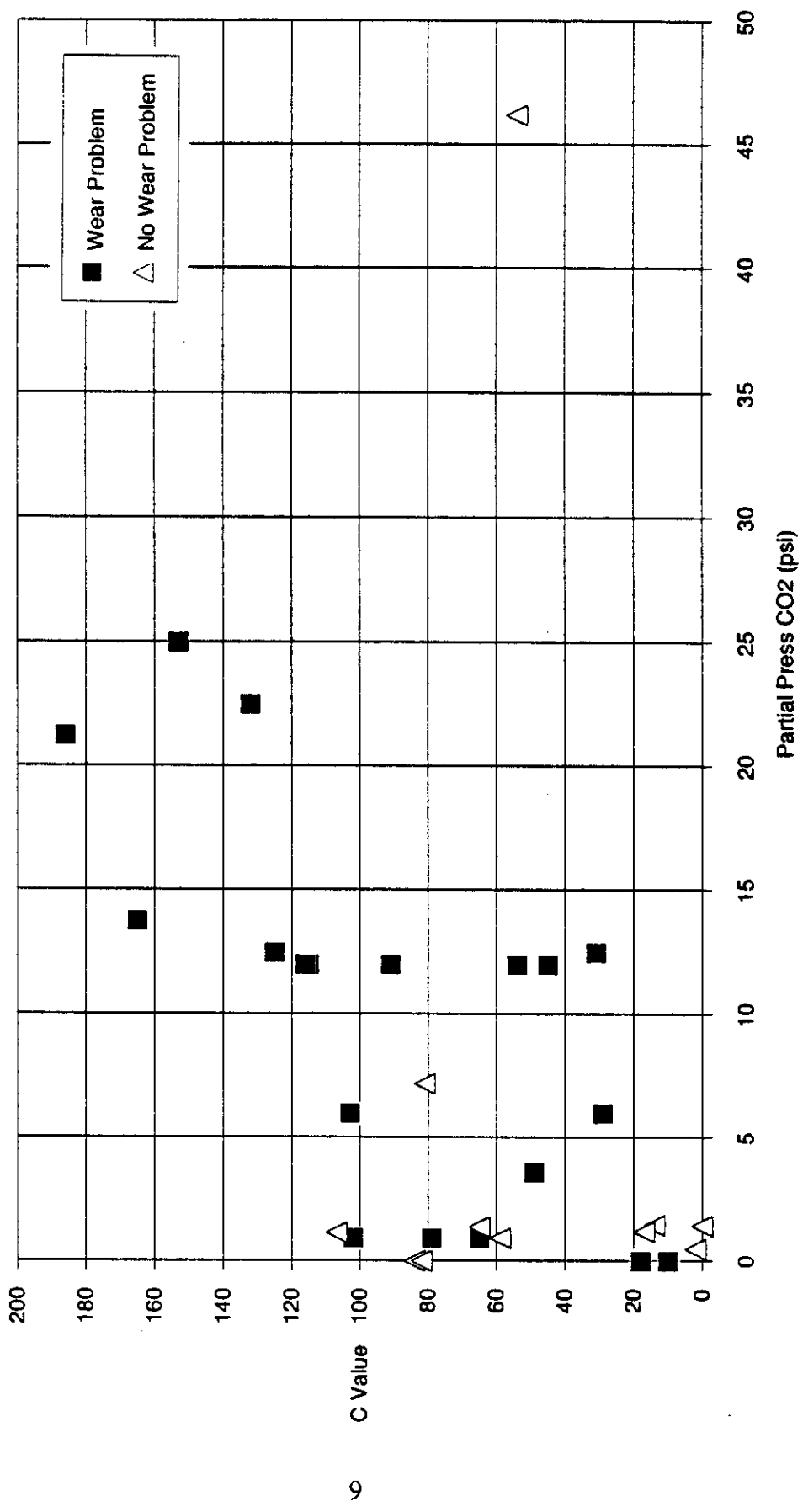


Figure 2.2 Plot of Actual "Operating" C-value (calculated from operating data) and CO<sub>2</sub> Partial Pressure

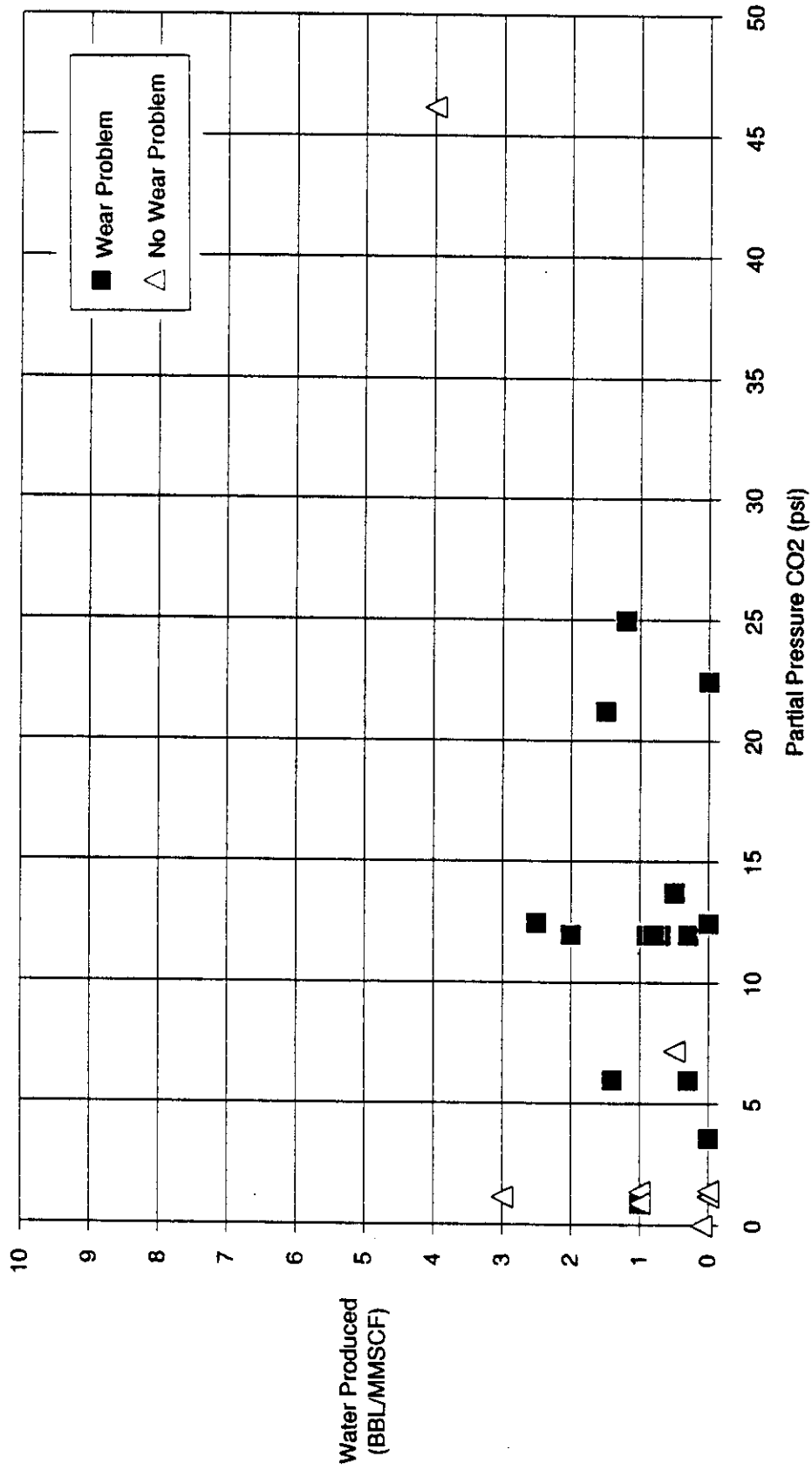


Figure 2.3 Plot of Water Production versus CO<sub>2</sub> Partial Pressure

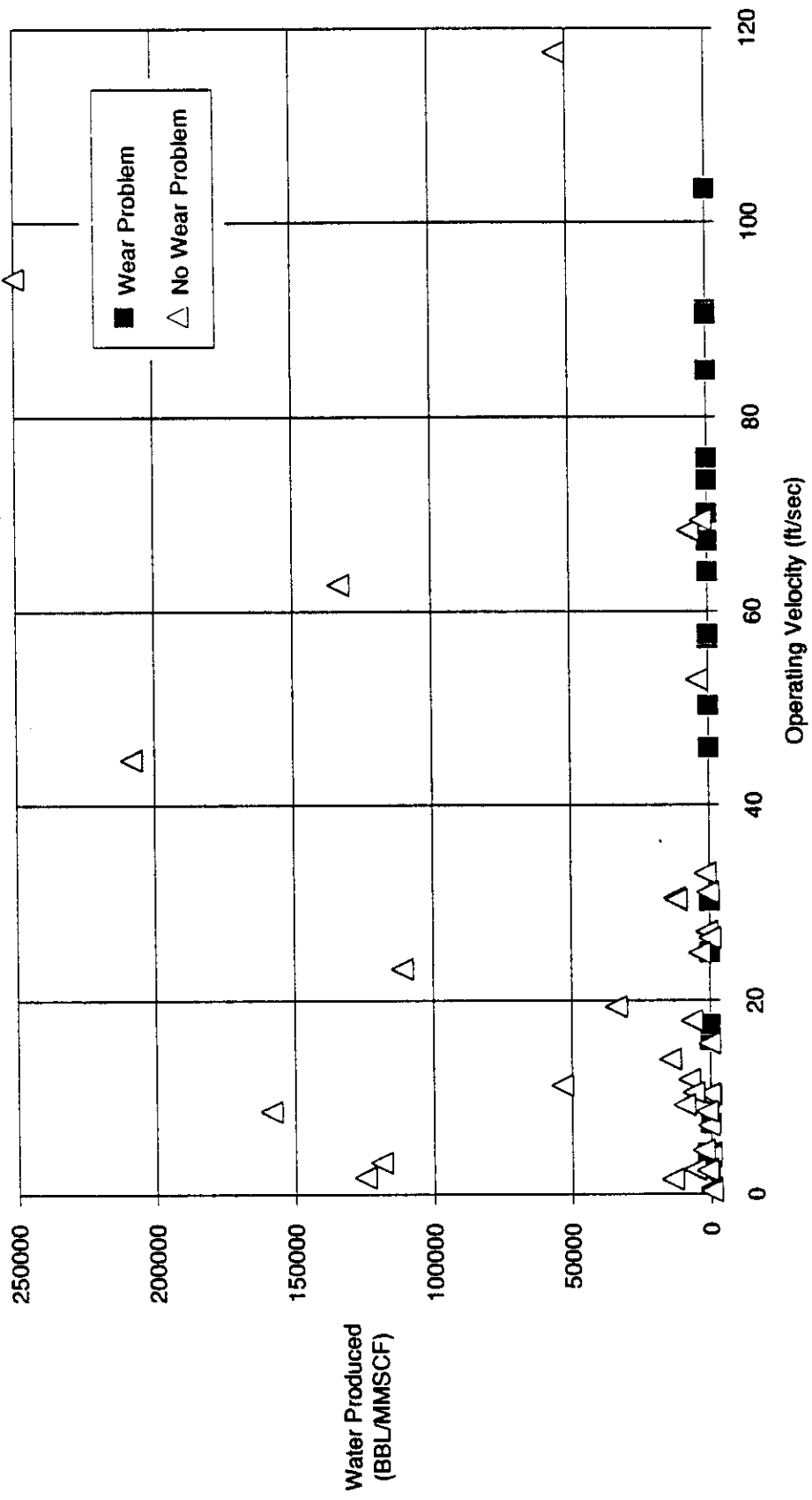
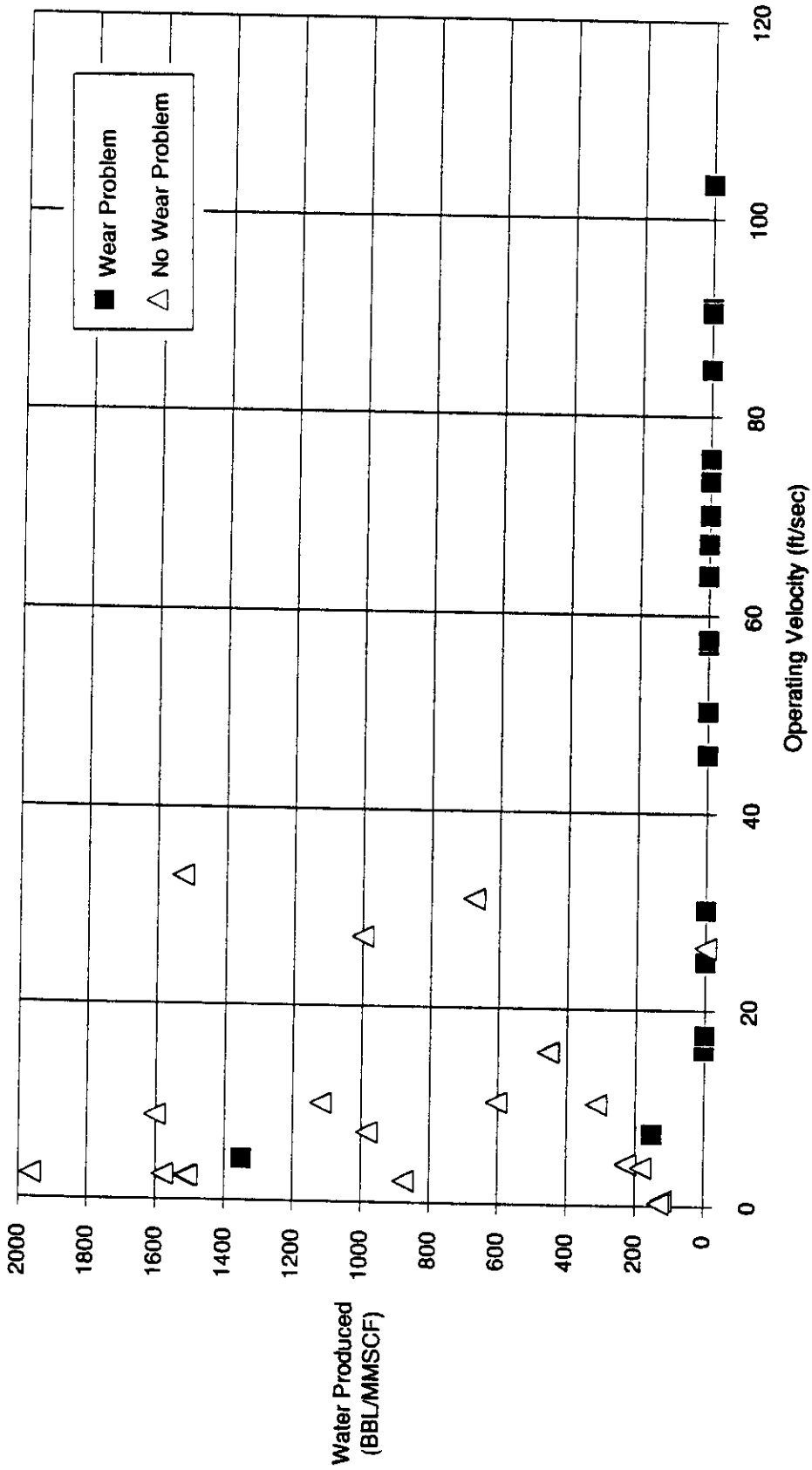


Figure 2.4 Plot of Water Production versus Operating Velocity



**Figure 2.5 Plot of Water Production on an Expanded Scale versus Operating Velocity**

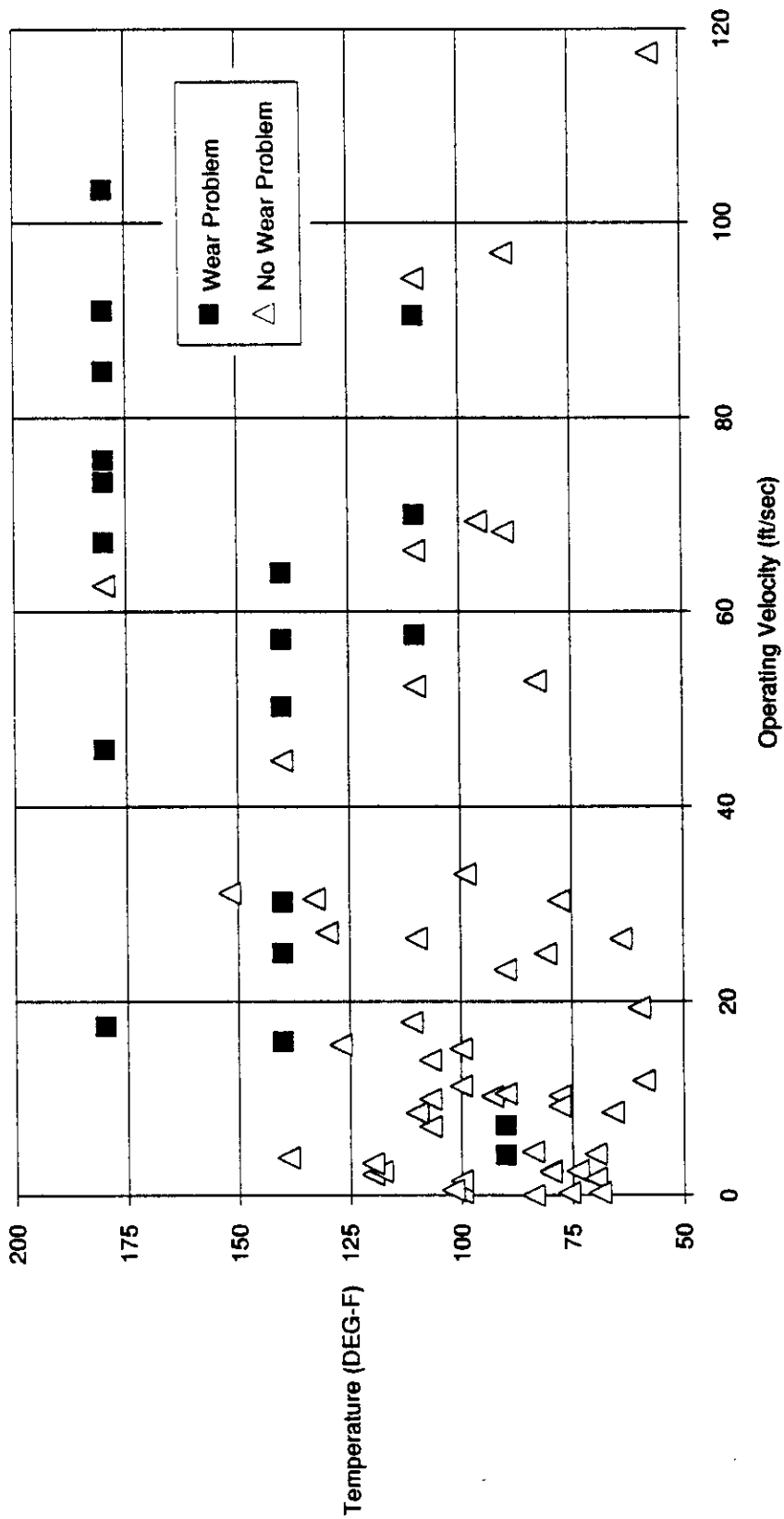


Figure 2.6 Plot of Operating Temperature versus Velocity

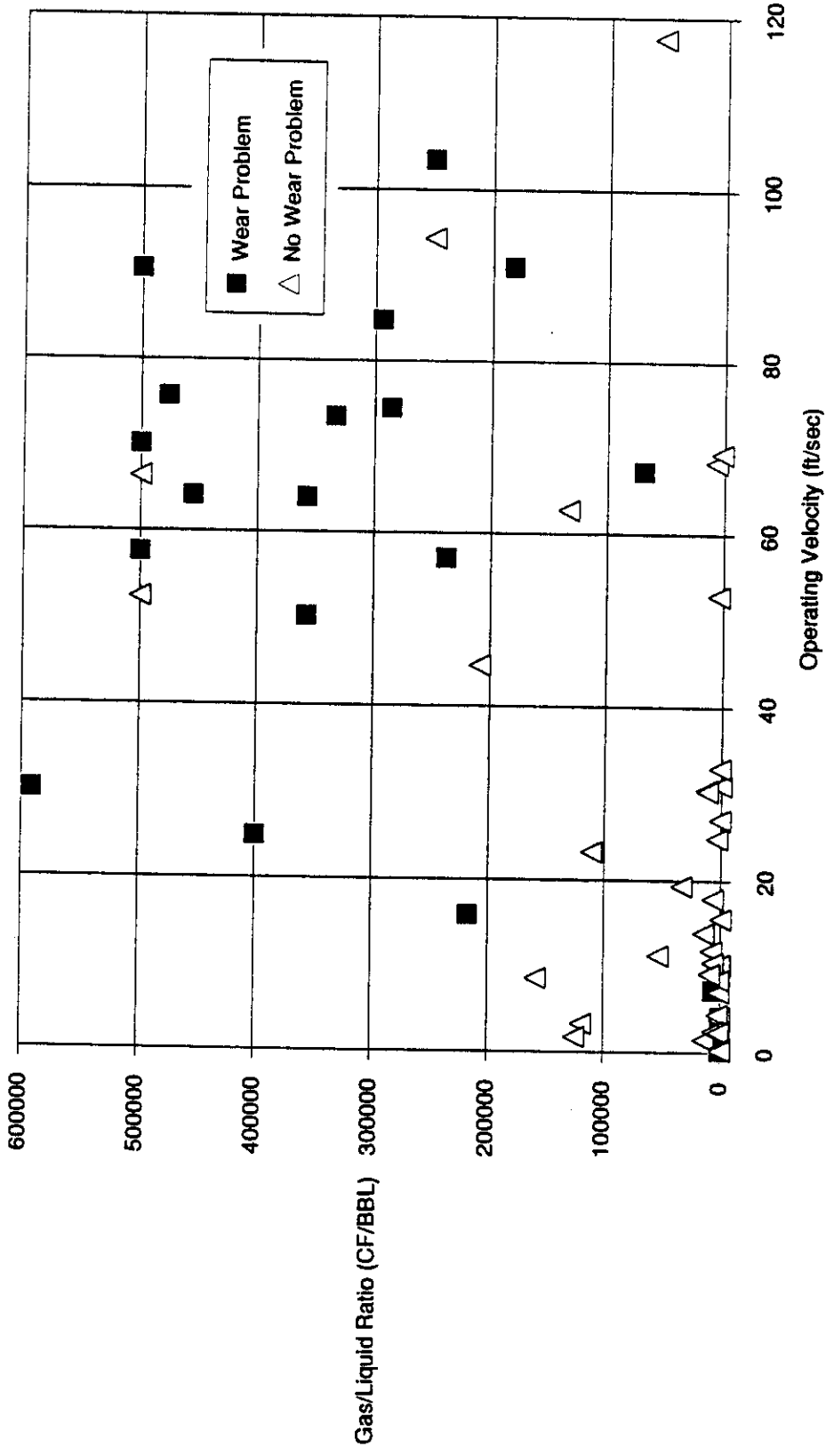


Figure 2.7 Plot of Gas to Liquid Ratio versus Operating Velocity

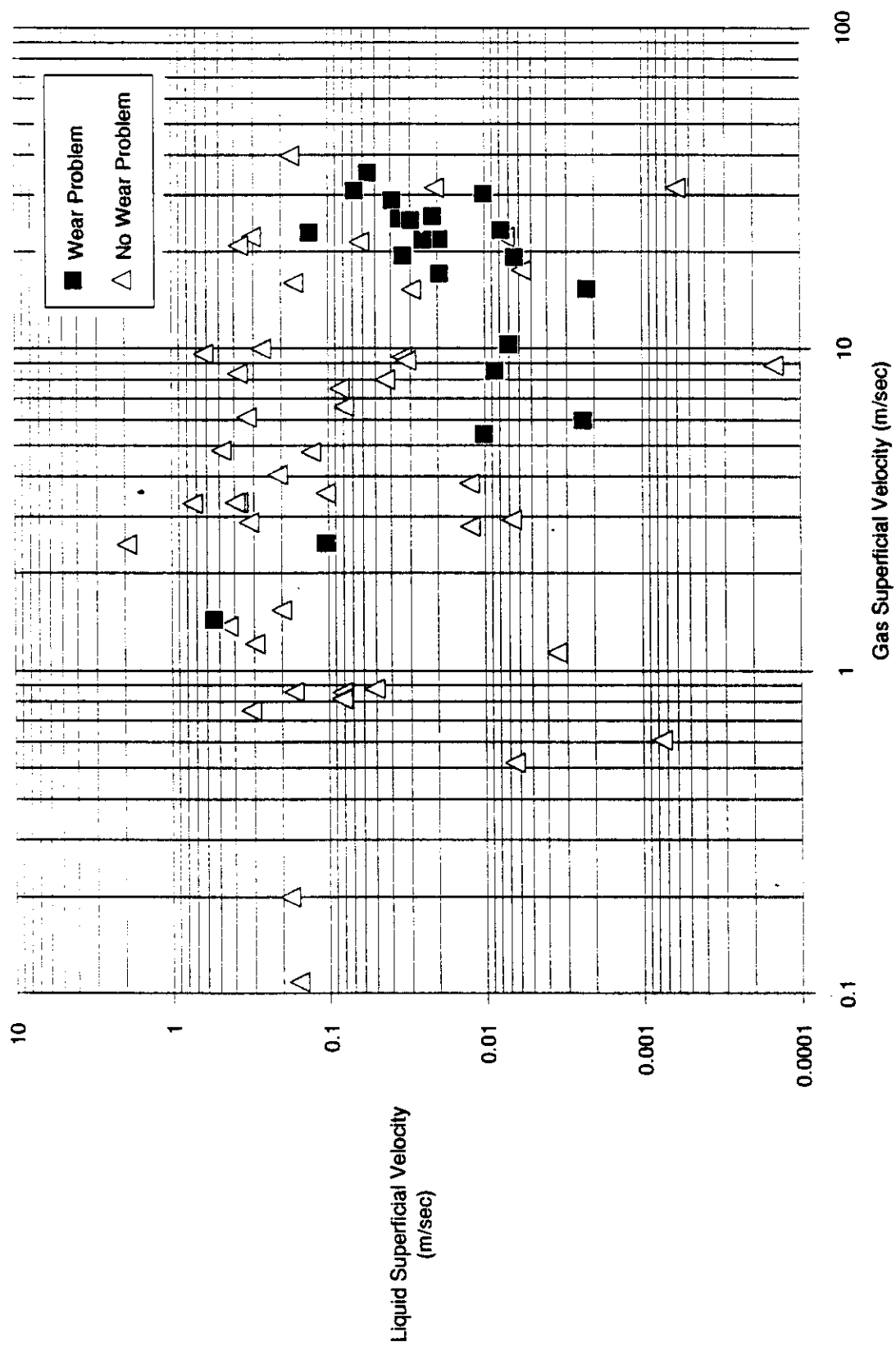


Figure 2.8 Plot of Superficial Gas Velocity versus Superficial Liquid Velocity

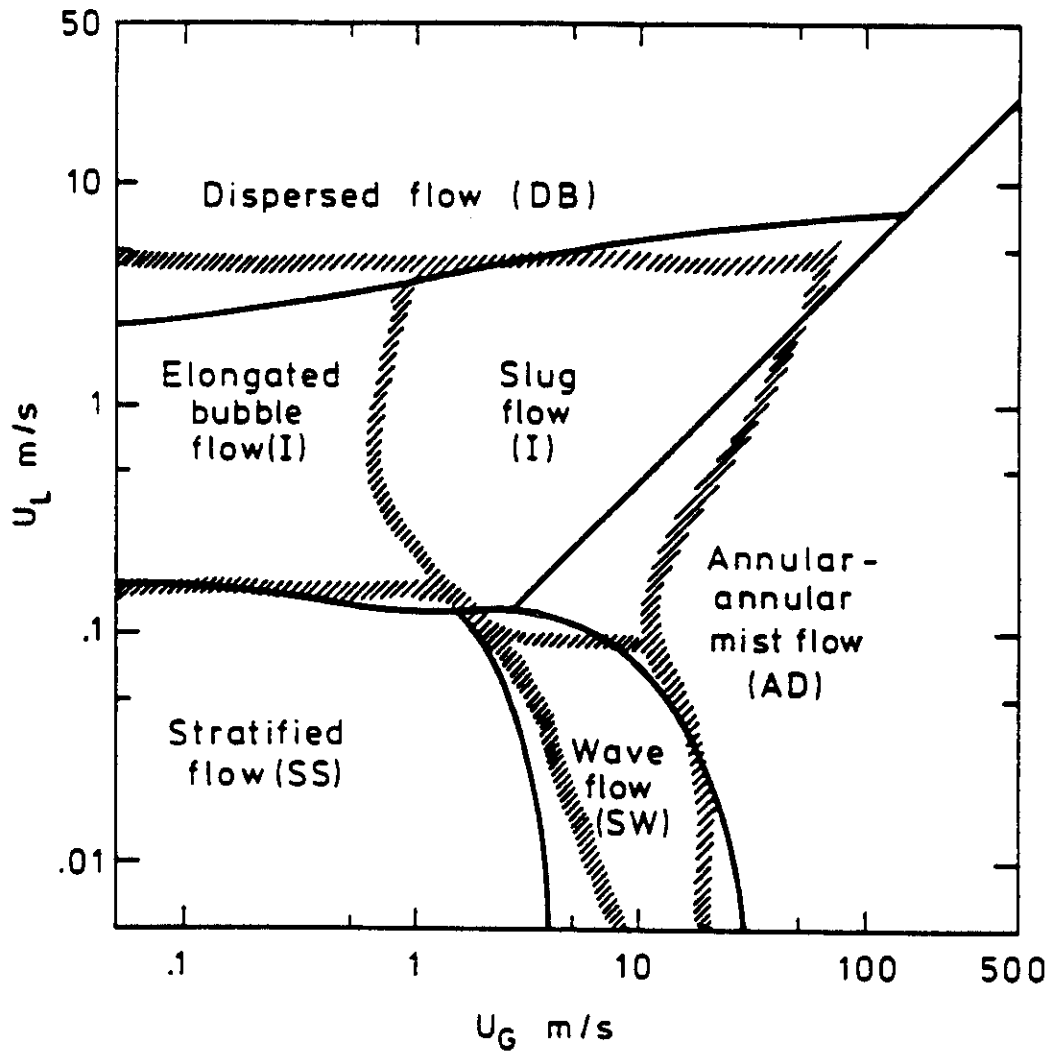


Figure 2.9 Flow Regime Boundary Map for Horizontal Pipe Showing Taitel and Dukler [5] and Mandhane et al [6] Boundaries



about 20 m/sec (and liquid velocity below 1.0 m/sec), the flow is in the annular or annular mist flow region. The data in this same region in Figure 2.8 shows a concentration of data points with wear problems. For the most part, the data points with wear problems are in the annular-mist region or close to the boundary in the wave flow region.

The two data points indicating wear problems at the lowest gas velocity have sand reported in the fluid. This may be the cause of the accelerated wear at a relatively low velocity. With the exception of these two points, Figure 2.8 clearly shows a correlation of flow regime with wear problems.

### 2.2.2 Data Set 2

In addition to the above data, three other companies responded to the request for erosion/corrosion data. The data is for a variety of pipe sizes, flow rates, corrosive conditions, and fitting types. A summary of the data is presented in Table 2.2. The wear rates reported varied from 0 to 3012 Mills Per Year (MPY) with the majority being less than or about 100 MPY. About 1/3 of the wear rates shown are below the "acceptable" wear rate of 5 MPY while all but two of the reported flow rates were below the erosional velocity limit set in API RP 14E (using  $C = 100$ ).

The two highest wear rates shown in Table 2.2 (3012 and 1106 MPY) were the only points that reported the presence of  $H_2S$ . They also both contained  $CO_2$  and the wear was reported for elbows. That is all that was common between the two high wear rate points. The pressures for these two points were the highest (4000 psig) and the lowest (40 psig); the pipe sizes were 4" and 10"; one operated at 95% below the erosional velocity and one 20% above it; one had a gas/liquid ratio of 35 while the other had a ratio of 10; and one had sand production and the other did not. From these two points, it is obvious that limiting the erosional velocity (based on the fluid mixture density only) is not an effective method of wear prevention when many different wear mechanisms are involved.

The next highest wear rate point reported was the failure of a 2" x 6" expansion section downstream of a choke with a wear rate of 450 MPY. The velocity was significantly less than the erosional velocity (based on the 6" pipe diameter), but the fluid velocities are obviously higher in the region of the expansion. For this point,  $CO_2$  was present in the gas, very little liquid was present with a gas/liquid ratio of 553,000, and the pressure was one of the highest reported at 1100 psig. The rest of the points summarized in Table 2.2 had considerably lower wear rates than the above discussed points.

Table 2.2 Summary of Field Data Operating Conditions

Pipe Diameter (inches)	Fitting Schedule	Fitting Type	Gas Flow (MSCFD)	Oil Flow (BBL/day)	Water Produced (BBL/BBL-oil)	CO2	H2S	Pressure (psig)	Temperature (F)	Sand (y/n)	Wear Rate (MPY)	Gas/Liquid Ratio (SCF/BBL)	Mixture Density (lbm/ft <sup>3</sup> )	Erosional Velocity (ft/sec)	Avg. Operating Velocity (ft/sec)	Water Flow (BPD)
2	80	90 Elbow	100	61	20	y	n	200	99,999	n	2.7	78	30,96	18.0	8.2	1220
2	80	90 Elbow	80	67	3	y	n	180	99,999	n	7.1	299	11,79	29.1	4.5	201
2	80	90 Elbow	133	180	5.6	y	n	235	99,999	n	1.3	112	27,40	19.1	8.5	1008
2	80	90 Elbow	120	67	9	y	n	330	99,999	n	23.3	179	25,60	19.8	5.2	603
3	80	90 Elbow	330	183	4	y	n	540	99,999	n	5.3	361	22,51	21.1	3.7	732
2	80	Tee	147	103	0.6	y	n	400	99,999	n	0.8	892	9,13	33.1	3.7	61.8
2	80	Tee	119	80	1	y	n	200	99,999	n	5.6	744	5,98	40.9	5.5	80
2	80	Tee	142	80	0.9	y	n	200	99,999	n	2.0	934	4,96	44.9	6.4	72
2	80	Tee	153	123	0.1	y	n	200	99,999	n	4.4	1131	4,03	49.8	6.8	12.3
2	80	Tee	282	135	0.05	y	n	200	99,999	n	1.6	1989	2,62	61.8	12.2	6.75
2	80	Tee	283	67	3.1	y	n	300	99,999	n	2.0	1030	6,77	38.4	8.9	207.7
2	80	Tee	46	104	0.4	y	n	250	99,999	n	0.0	316	13,42	27.3	2.0	41.6
2	80	90 Elbow	115	81	0.3	y	n	250	99,999	n	9.3	1092	5,14	44.1	4.2	24.3
2	80	Tee	123	25	0.1	y	n	250	99,999	n	0.0	4473	1,92	72.1	4.2	2.5
2	80	90 Elbow	23	8	10	y	n	430	99,999	n	3.7	261	24,06	20.4	0.7	80
2	80	90 Elbow	253	303	2.3	y	n	440	99,999	n	4.3	253	24,08	20.4	8.1	696.9
2	80	90 Elbow	97	13	9	y	n	315	99,999	n	5.0	746	9,23	32.9	3.0	117
2	80	90 Elbow	27	77	5.7	y	n	210	99,999	n	6.0	52	37,14	16.4	2.7	438.9
2	80	90 Elbow	67	123	5.4	y	n	220	99,999	n	5.7	85	30,53	18.1	5.0	664.2
2	80	90 Elbow	240	333	0.3	y	n	190	99,999	n	11.0	554	6,97	37.9	11.9	99.9
4	80	90 Elbow	32.2	920		y (3%)	y (12%)	4000	178	n	3012.0	35	51,94	13.9	0.8	0
4	80	Tee	150	180	1			174,999	99,999	n	46.5	417	8,55	34.2	2.1	180
2	80	Short Elbow	100	200	2.5			175	80	y	22.9	143	20,03	22.3	6.8	500
2	80	Tee	580	100	5.75			125	100		27.2	859	3,74	51.7	39.2	575
2	80	Tee	500	100	3			125	80		92.4	1250	2,81	59.7	32.1	300
2	80	Tee	335	140	2.5			175	80		198.8	684	6,10	40.5	16.8	350
2	80	Tee	550	270	1.57			175	100		109.3	793	5,15	44.1	28.1	423.9
2	80	Tee	375	120	3.33			175	100		48.2	722	5,69	41.9	19.3	399.6
2	80	Tee	500	100	3			125	80		81.5	1250	2,81	59.7	32.1	300
2	80	Tee	275	125	2.4			125	80		124.4	647	4,81	45.6	18.3	300
2	160	Elbow	300	30	46.7			150	99,999	n	70.0	210	13,97	26.8	27.4	1401
10	40	Long Elbow	1000	15000	5.67	n	n	40	195	n	1106.1	10	38,15	16.2	19.0	85050
6	120	2x6 Expan	25000	40	0.13	y (1.75%)	y (600ppm)	1100	120	n	449.6	553097	3,41	54.2	25.8	5.2

Notes:  
 (1) XXX,999 indicates estimate when value not provided.  
 (2) Calculations neglect gas compressibility.  
 (3) Assumed oil S.G. = 0.85 and gas S.G. = 0.65.

Since it is difficult to determine if any trends are apparent in the wear data in a table format, several plots from the data in Table 2.2 were made. Figure 2.10 shows the wear rate plotted against the operating velocity. The data show considerable scatter, but there is a trend of higher wear with higher operating velocity. Average flow velocities below 15 ft/sec have wear rates below 30 MPY (with the exception of one point showing very high wear) with the wear rate well in excess of 30 MPY at operating velocities above 15 ft/sec. Figure 2.11 shows the erosional velocity limit (from API RP 14E with  $C = 100$ ) plotted against the average operating velocity. The plot shows most of the flow lines are operating well below the erosional velocity limit. While the erosional velocity limit may be considered conservative for some applications, these two plots show that it is far from conservative when corrosion is involved. Figure 2.12 summarizes this by plotting wear rate against the ratio of the actual operating velocity to the erosional velocity. Only two points are above the erosional velocity (that is, the ratio is greater than one) and many of the points show excessive wear.

The effect of the presence of water in a flow line on the wear rate is shown in Figure 2.13. The data show considerable scatter with no clearly defined trend. Figure 2.14 shows wear as a function of gas/liquid ratio. Here again, no firm trend is apparent due to the scatter in the data. Figures 2.15 and 2.16 show the wear rate plotted against gas and liquid superficial velocities.

Figure 2.17 shows the data plotted as superficial gas velocity against superficial liquid velocity. The velocity units are in m/sec so a direct comparison can be made with the flow regime boundary map given in Figure 2.9. Since most of these points are below the erosional velocity limit, they are below the boundary line (in Figure 2.9) for transition into annular mist flow (the boundary to annular mist flow is at about 20 m/sec for gas superficial velocity, and the minimum mixture density for this data ( $1.9 \text{ lbm/ft}^3$ ) gives an erosional velocity of about 20 m/sec (72 ft/sec)). The majority of the data points with reported wear greater than 10 MPY are in the slug flow regime and most are close to the annular mist flow boundary.

One high wear point (solid square symbols) falls in the stratified flow regime (point furthest to the left in Figure 2.17). This point was for wear (47 MPY) in a tee and had sand in the flow stream. The high wear point in the wave flow region (with the lowest liquid superficial velocity) was an expansion from 2-inch to 6-inch pipe with very little liquid flow. The gas superficial velocity plotted for this point is based on the 6-inch pipe, but the local velocity at the expansion is obviously much higher. This means the flow was probably annular mist flow and that caused the high wear rate (450 MPY) reported for this point.

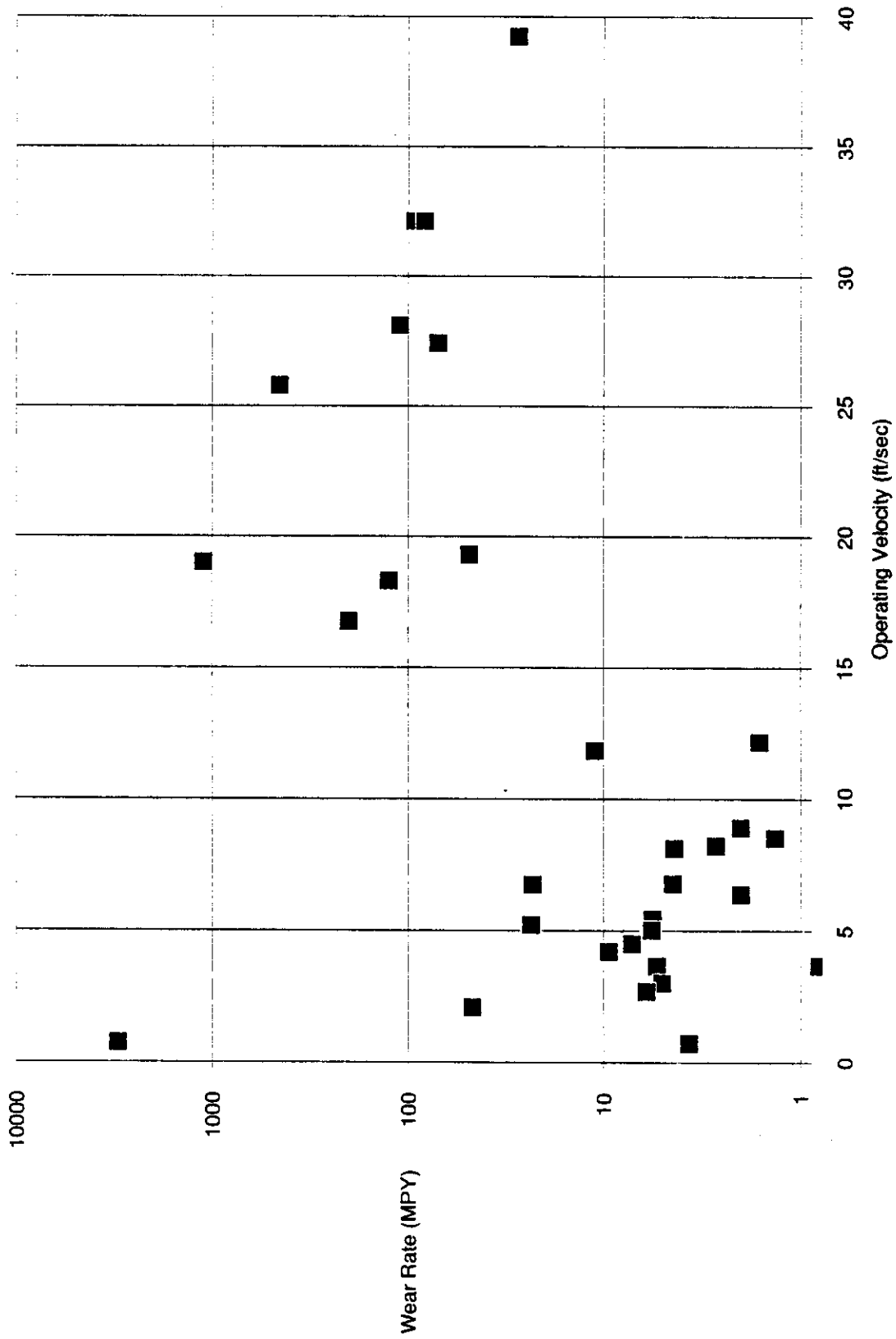


Figure 2.10 Plot of Wear Rate versus Operating Velocity

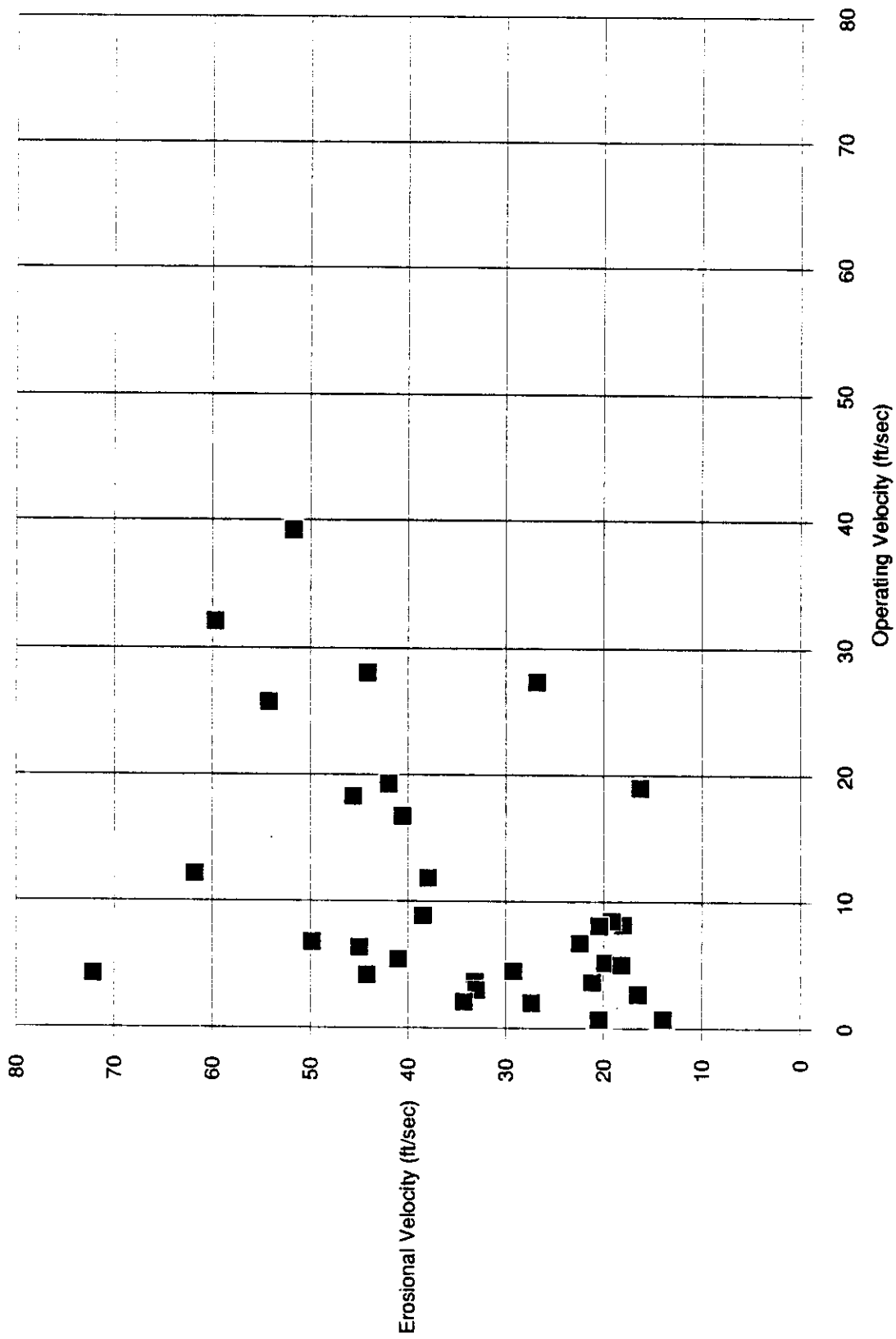


Figure 2.11 Plot of Erosional Velocity versus Actual Operating Velocity

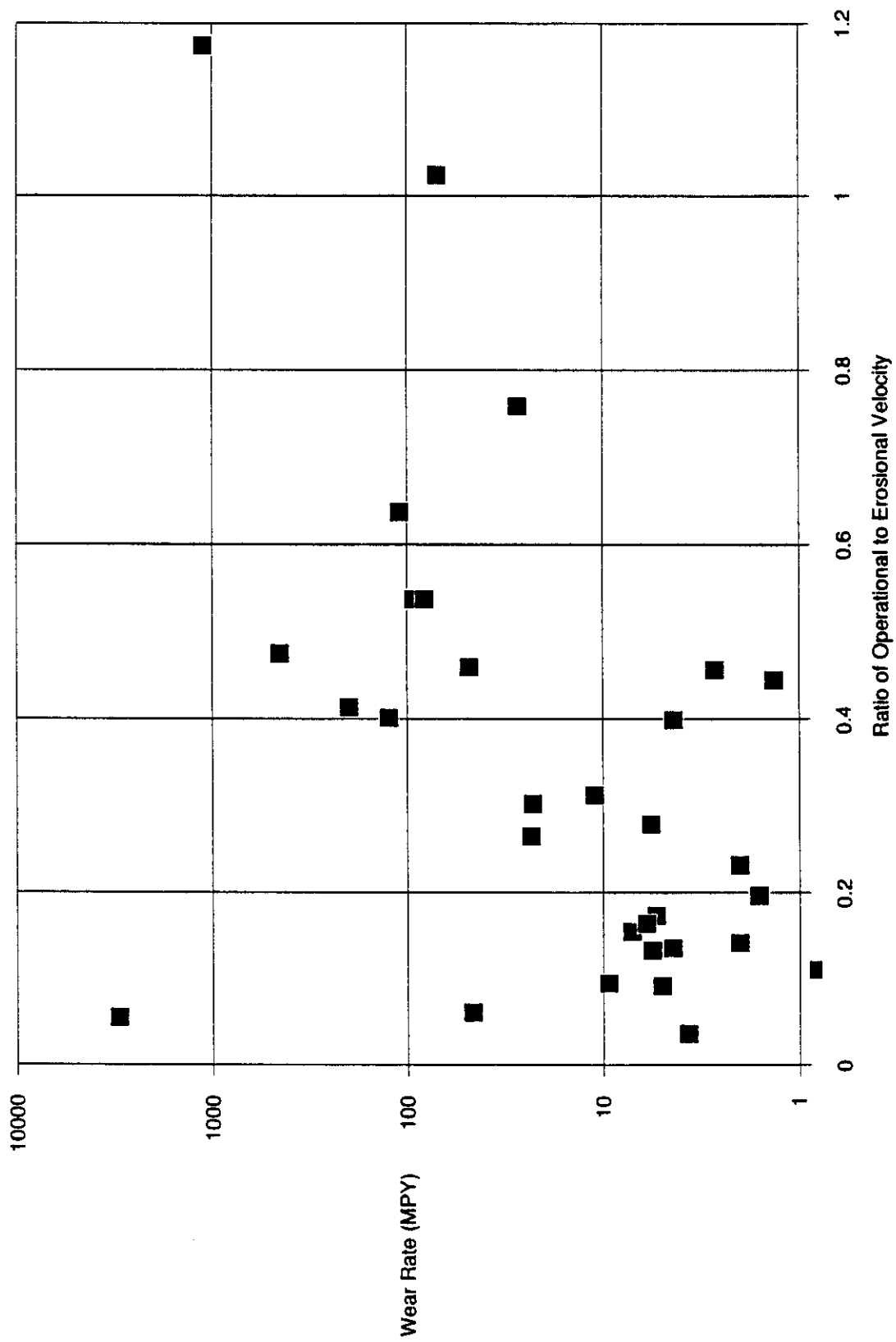


Figure 2.12 Plot of Wear Rate versus Ratio of Actual Operating Velocity to Erosional Velocity

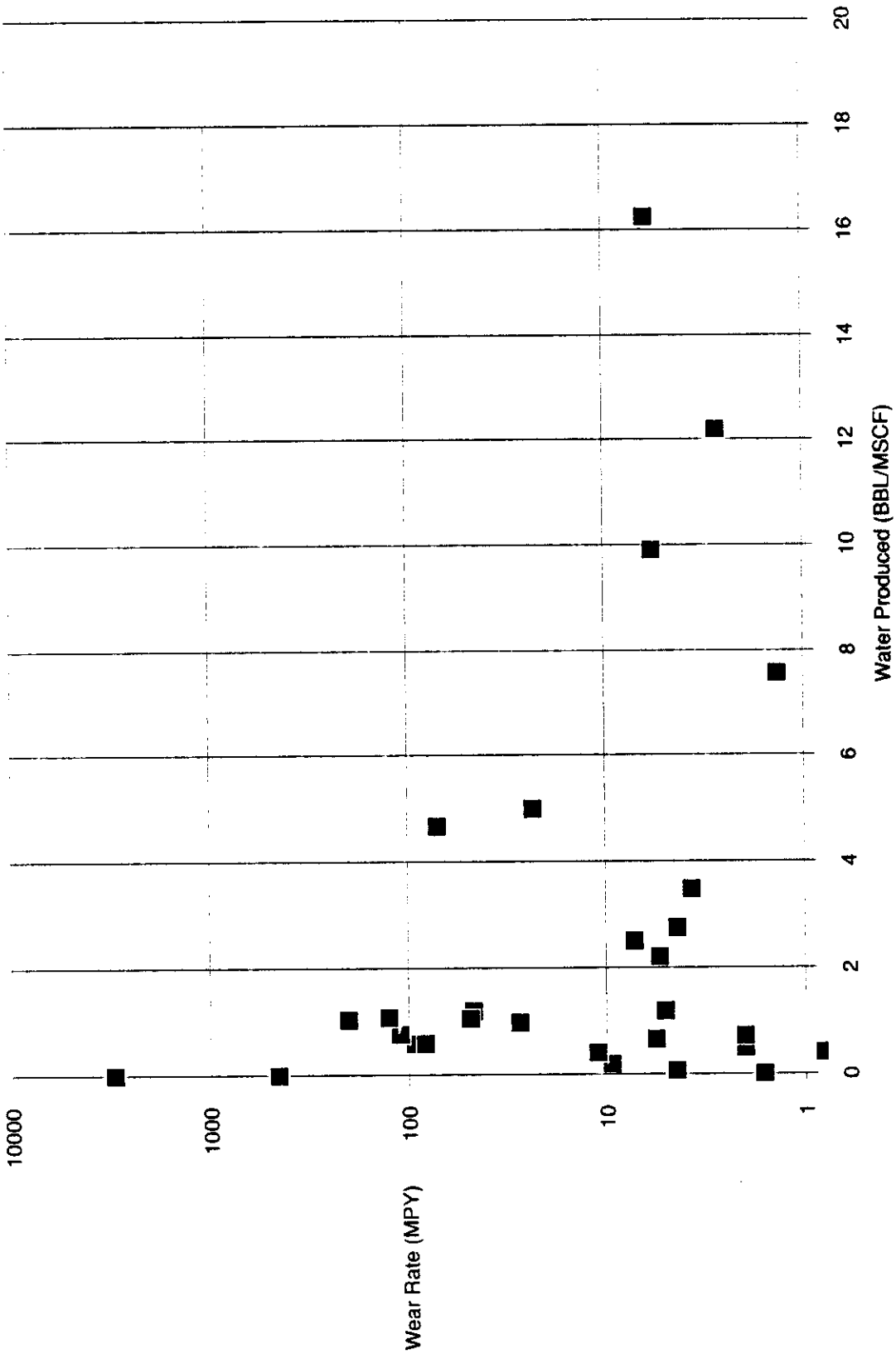


Figure 2.13 Plot of Wear Rate versus Water Production

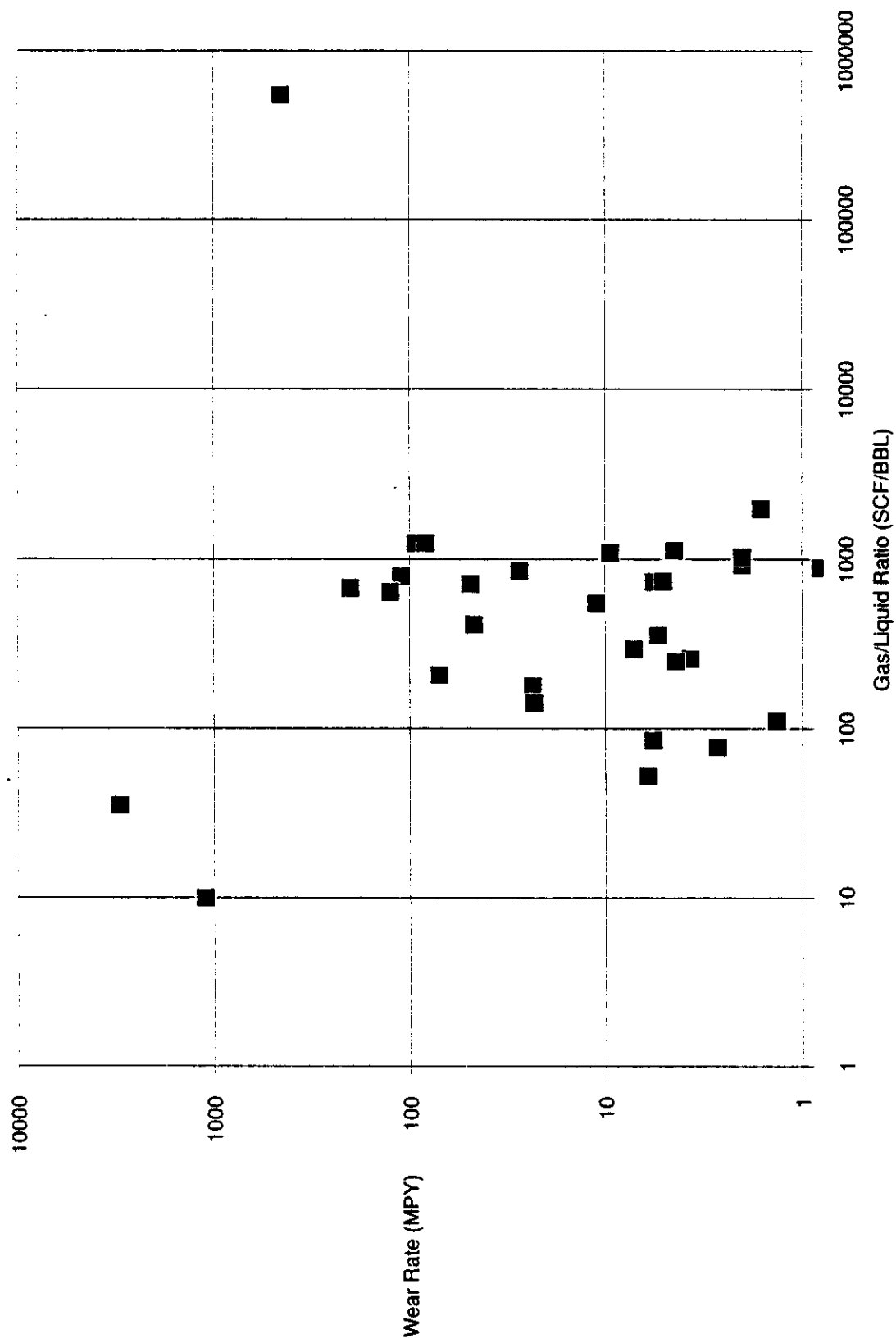


Figure 2.14 Plot of Wear Rate versus Gas to Liquid Ratio



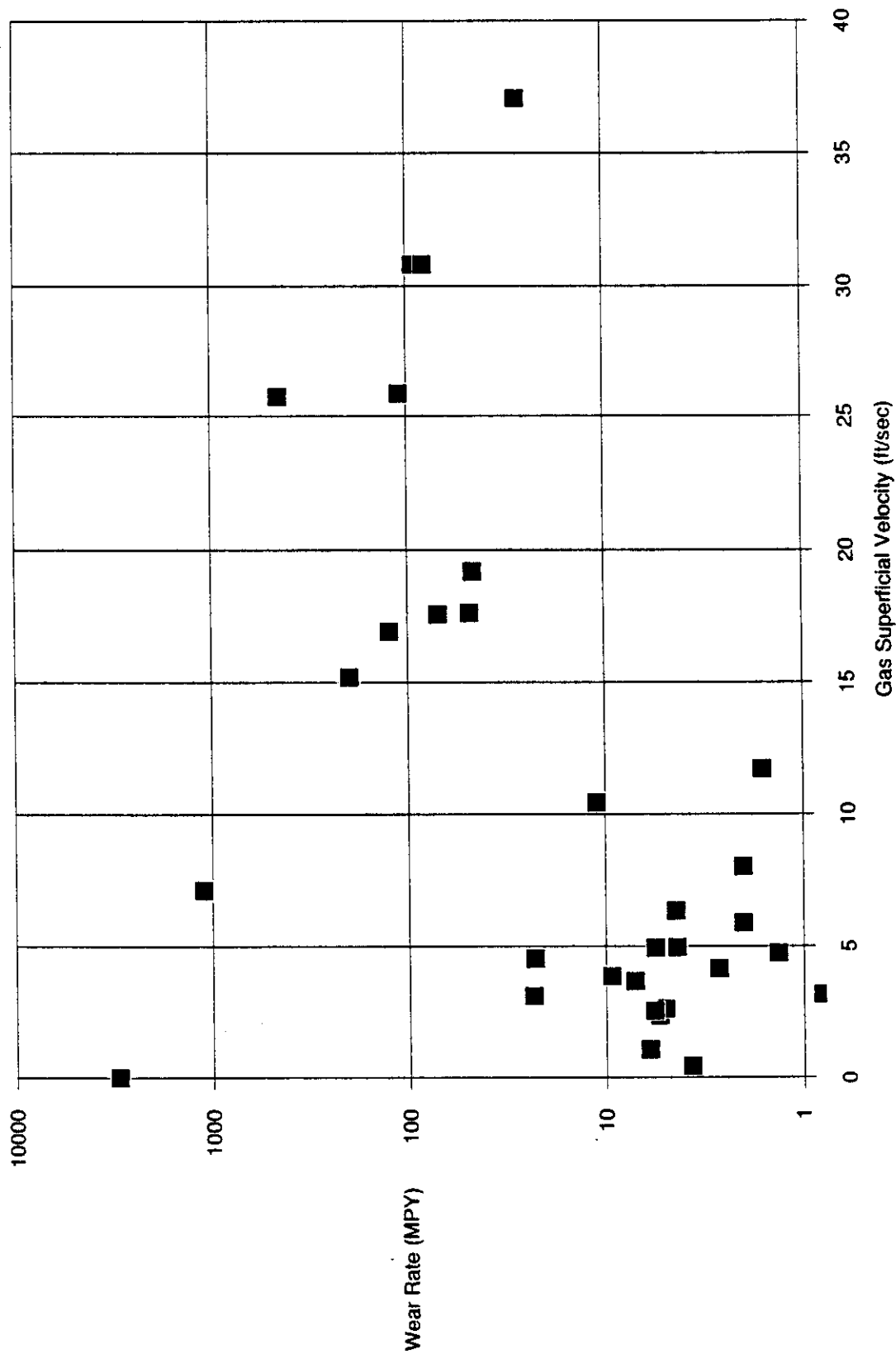


Figure 2.15 Plot of Wear Rate versus Gas Superficial Velocity

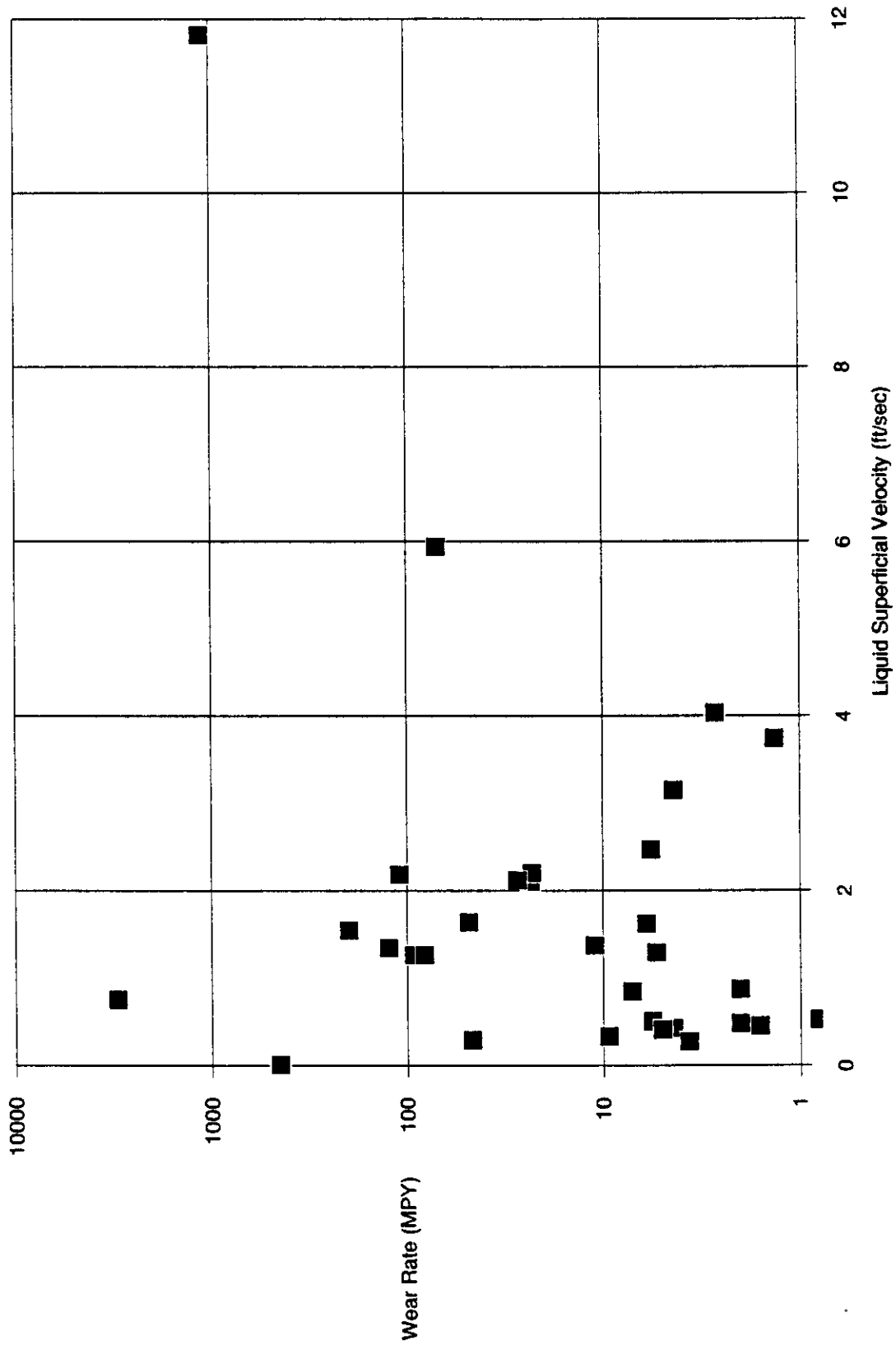


Figure 2.16 Plot of Wear Rate versus Liquid Superficial Velocity

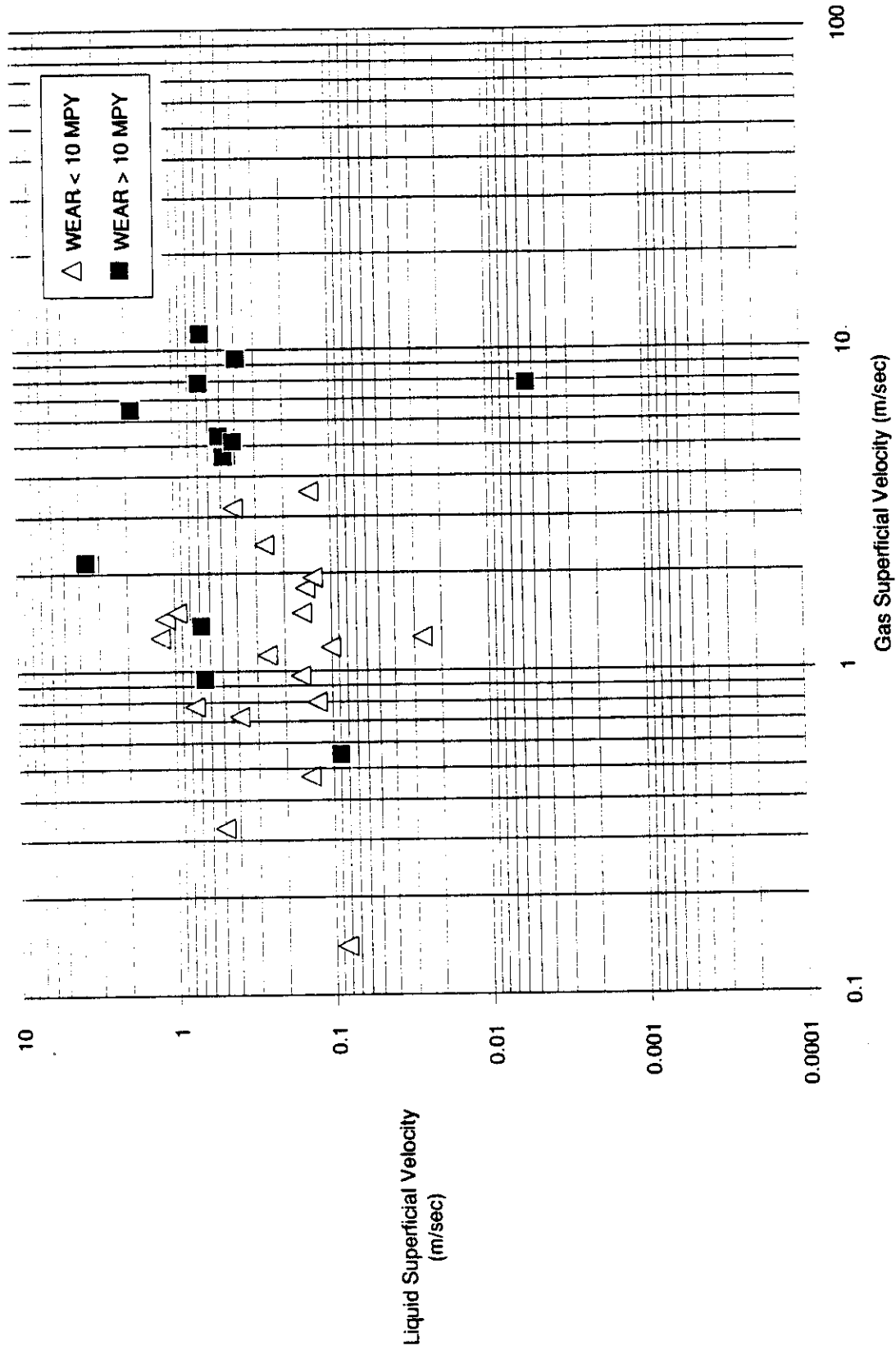


Figure 2.17 Superficial Gas Velocity versus Superficial Liquid Velocity

### **3.0 ADDITIONAL EROSION/CORROSION DATA**

#### **3.1 Erosion/Corrosion Study of Solids Free Gas Wells**

Duncan [7] reported the results of wear measurements made over a ten year period in gas wells in Bahrain. The gas contained 6 mole percent CO<sub>2</sub> and 0.06 mole percent H<sub>2</sub>S. Very severe wear (in excess of 100 MPY) was reported when the carbon steel piping was initially operated at a velocity of 44 ft/sec. During the first eight months of well operation, the pipe downstream of the choke in a well operating at 38 ft/sec suffered local wear rates from 44 to 177 MPY. These severe wear rates were seen again when the permanent manifold lines were installed at the wells. After two years of operation, the maximum corrosion rates at 45° elbows and tees was 91 MPY in a line operating at 59 ft/sec and 43 MPY in a line operating at 46 ft/sec. These wear rates were seen even though the permanent manifolds were continuously injected with an amine inhibitor at the well head. Significantly reduced wear was observed in the larger piping manifold (6") downstream (that operated at 16 to 23 ft/sec) of the above described lines with wear of only 4 MPY.

When flow rates in the two lines was reduced to 31 and 39 ft/sec, the corrosion rates (over the next 2 years) at bends and tees was 28 MPY for the lower velocity line and 55 MPY for the higher velocity line. Figure 3.1 summarizes the wear rates experienced in several wells. From this figure, it can be seen that a threshold for accelerated wear occurs at about 29 ft/sec (9 m/sec) for the inhibited piping. Very little data is available on uninhibited piping, but, as expected, accelerated wear occurs at lower operating velocities compared to inhibited piping. Figure 3.1 also shows that straight sections wear at about 1/2 to 1/4 the rate of tees and elbows.

Duncan reported that wear rates were generally less than 8 MPY for inhibited systems operated at velocities up to 20 ft/sec. Wear in the straight sections was even lower than this. At velocities of 30 to 40 ft/sec, the wear rates very rapidly became unacceptably high. Duncan felt the critical velocity was due to either the inhibitor film or corrosion products were no longer able to provide protection to the pipe surface, or a flow transition from annular to mist flow occurred. Since very little sand was present in the wells, the wear rates reported were primarily caused by corrosion. Duncan reported there were no problems with H<sub>2</sub>S stress corrosion cracking in the carbon steel pipe or fittings where hardness was kept within NACE Specifications.

#### **3.2 Erosion in Blow-Out Prevention Systems**

Bourgoyne [8] did a detailed study of fitting erosion in blow-out prevention systems used in offshore drilling. He measured fitting erosion rates caused by sand flow in dry gas, wet gas, and liquid flows. A number of different fitting geometries were evaluated.

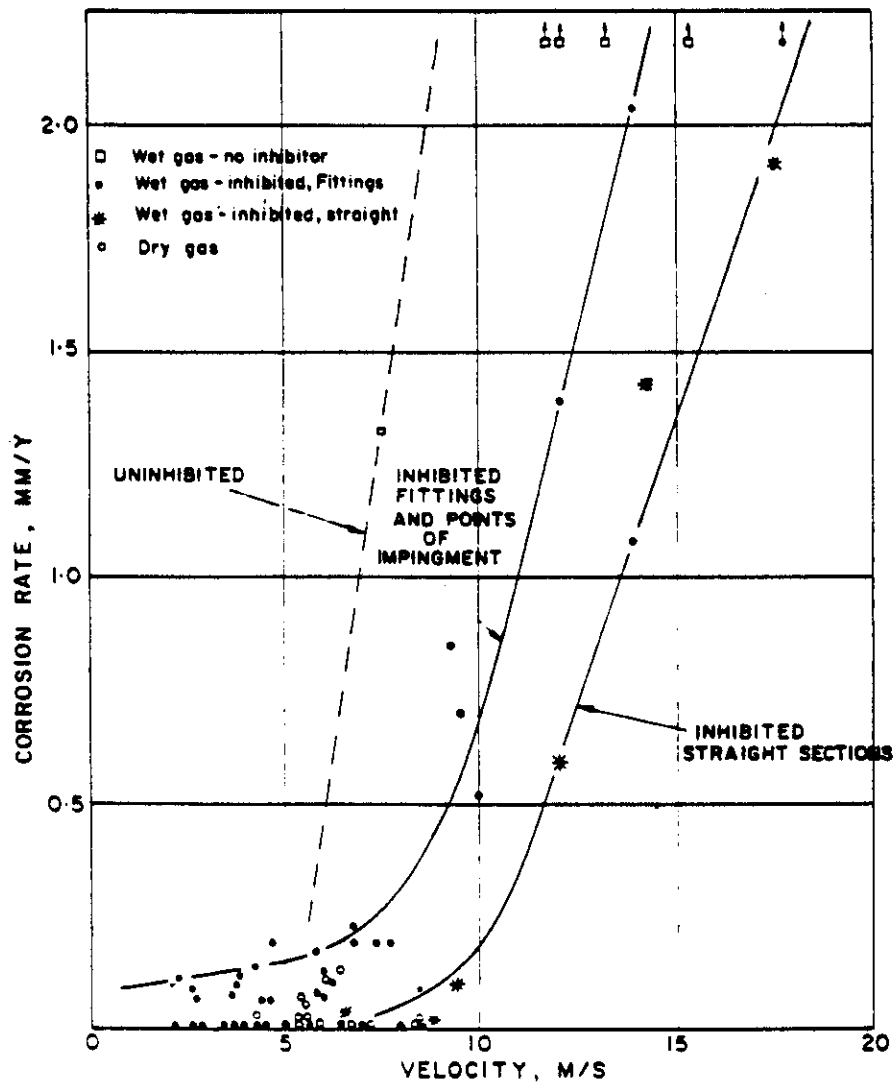


Figure 3.1 Results of Corrosion Measurements by Duncan [7]

Bourgoyne found the erosion rate of sand in mud was one to two orders of magnitude lower than sand in air. Small quantities of water added to the air/sand mixture increased the erosion rate by 10 to 25%. Longer radius elbows showed less wear in the gas/sand mixtures, but the opposite was found in the liquid/sand mixtures.

Based on the experimental erosion data, Bourgoyne developed an equation to predict the wall loss rate in the fitting as a function of the specific erosion factor,  $F_e$ , density of the abrasive,  $\rho_a$ , density of pipe,  $\rho_s$ , gas or liquid superficial velocity,  $V_{sg}$  or  $V_{sl}$ , pipe cross-sectional area,  $A$ , volume fraction of gas or liquid  $\lambda_g$  or  $\lambda_l$ , and the abrasive flow rate,  $q_a$ :

$$\text{For dry gas or mist flow } -\frac{dh_w}{dt} = F_e \frac{\rho_a q_a}{\rho_s A} \left( \frac{V_{sg}}{100\lambda_g} \right)^2 \quad (\text{Eq. 3})$$

$$\text{For liquid flow } -\frac{dh_w}{dt} = F_e \frac{\rho_a q_a}{\rho_s A} \left( \frac{V_{sl}}{100\lambda_l} \right)^2 \quad (\text{Eq. 4})$$

The values for the specific erosion factor were tabulated for various elbow geometries, tees, flexible hose, and a vortice elbow. Bourgoyne's table is reproduced in Figure 3.2. Bourgoyne's specific erosion factor is the ratio of the mass of pipe material removed to the mass of abrasive through the fitting. The velocity dependence of the specific erosion factor is shown in Figure 3.3. The data in this plot is for erosion of an elbow (with a radius to diameter ratio of 1.5) by sand in air. The slope of 2 for the line drawn in the figure represents a wear dependence with velocity squared.

### 3.3 Laboratory Study of Fitting Erosion

Weiner and Tolle [9] ran erosion tests similar to the above described test by Bourgoyne. The tests were run to measure erosion rates in fittings due to sand flowing in air. Tests were conducted at velocities of 50, 70, and 100 ft/sec with sand flow at 3 lbm/min. This high sand flow rate caused accelerated erosion of fittings (an elbow would wear through in one day) so a number of tests could be performed in a short time. A variety of fitting geometries were tested including short and long radius elbows and plugged tees.

Weiner and Tolle found the wear rate in the fittings was proportional to the amount of sand through the fitting (that is, the data can be correlated with a "specific wear factor") and that the wear increased with flow velocity. Figure 3.4 shows their results from a test of "water elbows" (short radius elbows with radius to diameter ratio of 0.7) with a sand flow rate of 3.1 lbm/min and at three different velocities. Weiner and Tolle also ran three tests to determine the

### Recommended Values of Specific Erosion Factor

Cast Steel is ASTM 216, Grade WBC and Seamless Steel is ASTM A234, Grade WPB

Fitting Type	r / d	Material	Specific Erosion Factors ( g / kg )		
			Dry Gas Flow	Mist Flow	Liquid Flow
Ell	1.5	Cast Steel	2.2	2.8	0.001
		Seamless Steel	0.89	1.1	
	2.0	Cast Steel	2.0	2.4	0.001
		Seamless Steel	0.79	0.93	
	2.5	Cast Steel	1.7	2.0	0.001
		Seamless Steel	0.69	0.77	
	3.0	Cast Steel	1.5	1.65	0.0014
		Seamless Steel	0.60	0.66	
	3.5	Cast Steel	1.2	1.32	0.0076
		Seamless Steel	0.52	0.55	
	4.0	Cast Steel	0.9	1.0	0.01
		Seamless Steel	0.45	0.49	
	4.5	Cast Steel	0.7	0.77	0.01
		Seamless Steel	0.40	0.44	
	5.0	Cast Steel	0.5	0.55	0.01
		Seamless Steel	0.35	0.38	
Flexible Hose	6.0	Rubber	1.00	1.22	0.02
	8.0		0.40	0.45	
	10.0		0.37	0.39	
	12.0		0.33	0.35	
	15.0		0.29	0.31	
	20.0		0.25	0.28	
Plugged Tee	—	Cast Steel	0.026	0.064	0.0046
		Seamless Steel	0.012	0.040	0.01
Vortice Ell	3.0	Cast Steel	0.0078*		0.0028

\* Assumes Failure in Pipe Wall Downstream of Bend.

Figure 3.2 Specific Erosion Factors Given by Bourgoyne [8]

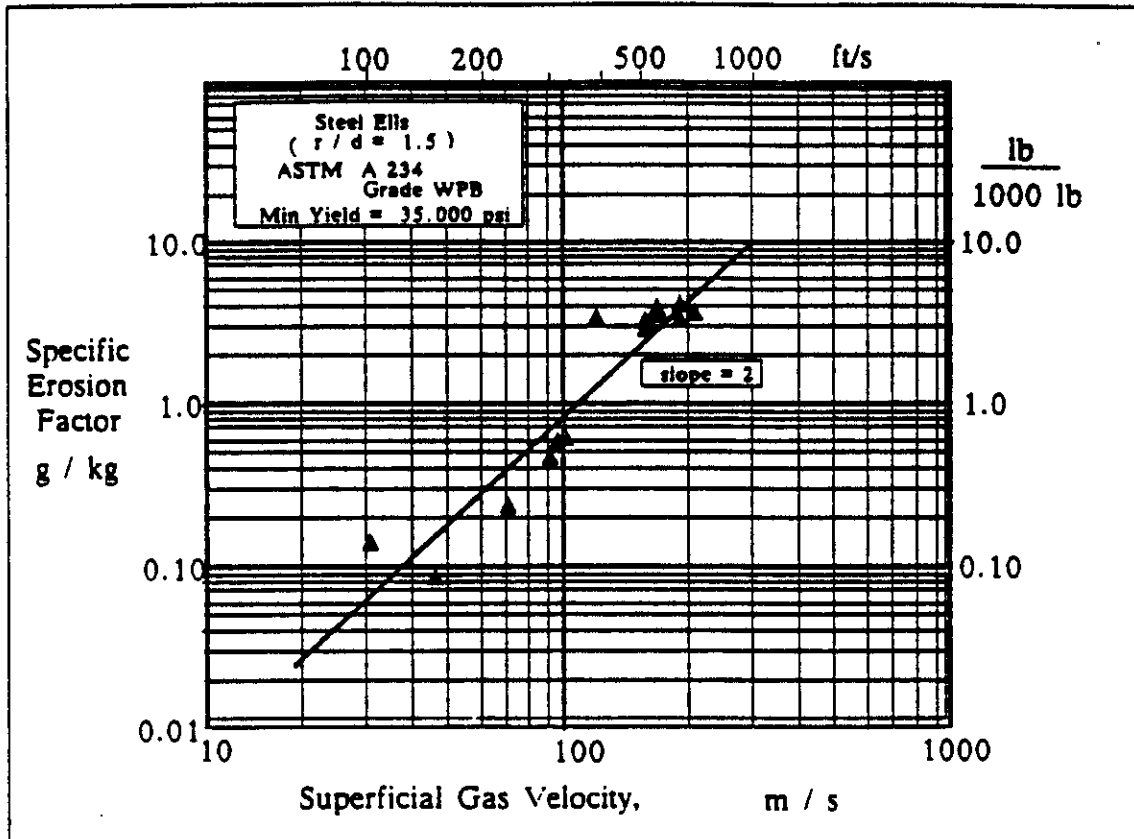
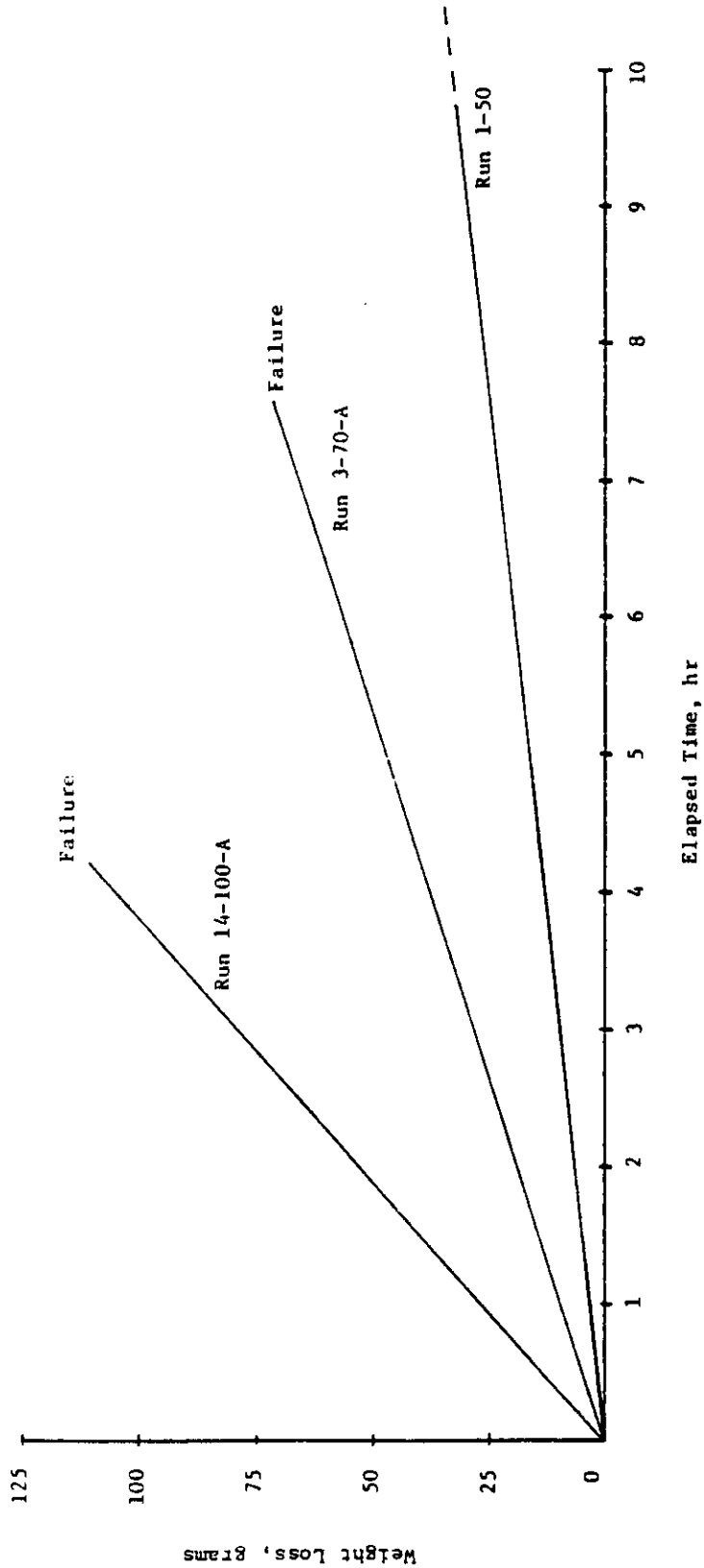


Figure 3.3 Wear Data on an Elbow Presented by Bourgoyne [8]





Weight Loss, grams vs. Elapsed Time, hr.  
 40/60 frac sand (dry)  
 90° ell of Run 1-50 did not fail. Test terminated  
 due to low wear rate

Weight Loss, grams = W

Elapsed Time, hr = t

Run 1-50 W = 3.18t Flow velocity 50 ft/sec

Sand Flow 3.09 lb/min

Run 3-70-A W = 9.26t Flow velocity 70 ft/sec

Sand Flow 3.10 lb/min

Run 14-100-A W = 26.78t Flow velocity 100 ft/sec

Sand Flow 3.11 lb/min

Figure 3.4 Wear Rates for a 90° Water Ell at Different Flow Velocities from Weiner and Tolle [9]

effect of sand flow rate on the fitting wear rate. The test results are shown in Figure 3.5. The three curve fit lines were for sand flow rates of 3.10, 2.87, and 2.44 lbm/min (all with a flow velocity of 70 ft/sec). The material loss for the 3.10 and 2.87 lbm/min sand rates were almost identical. The wear from the 2.44 lbm/min sand flow rate test was about half the other two. This result is difficult to interpret based on the limited test data. The trend seen here is different from what others have reported, that is, wear rate is independent of loading rate until interparticle interactions become important at higher particle concentrations (and then wear rate falls off).

Weiner and Tolle also ran a test to determine the effect of particle size on fitting wear. The test was run at a gas velocity of 70 ft/sec with two sizes of sand (16/20 and 40/60 mesh) with different sand flow rates. The larger diameter sand particles showed slightly less wear on a specific wear basis. Here again, the test was not conclusive since only one test was run for comparison.

The results of a comparison between different fitting geometries showed higher wear in shorter radius elbows compared to longer radius elbows, and still less wear measured in plugged tees. While a large number of tests were performed in the testing program, still more data is required before the effects of particle size, particle loading, fitting temperature, and fitting material can be determined.

#### 4.0 CONCLUSIONS

At the start of this project, it was hoped that enough field data would be available to determine the empirical constants ( $K$  and  $n$ ) in Equation 1 for at least a few different flow conditions and fitting types. As previously discussed, the quantity and quality of data initially anticipated was not available. Based on the available data, it became apparent that a single erosional velocity equation would not be sufficient to cover the variety of conditions encountered in the field. This is seen in the scatter in the data plotted as wear versus operating velocity. If a limiting wear rate could be correlated with this single parameter (erosional velocity (which is a function of density)), all the data would be separated into data showing excessive wear above the line and the data without wear problems below it. The data shows this is far from what actually happens because of the variety of factors that influence pipe wear.

In an attempt to limit the number of variables that must be considered, the following discussion is broken down into several categories. The first category is "clean" two-phase flow service. Because this type of flow does not involve solids or corrosion, a different form of the erosional velocity equation would be expected. The second category is erosive multiphase flows that include solids. Since corrosion is not important in this classification, the erosional velocity

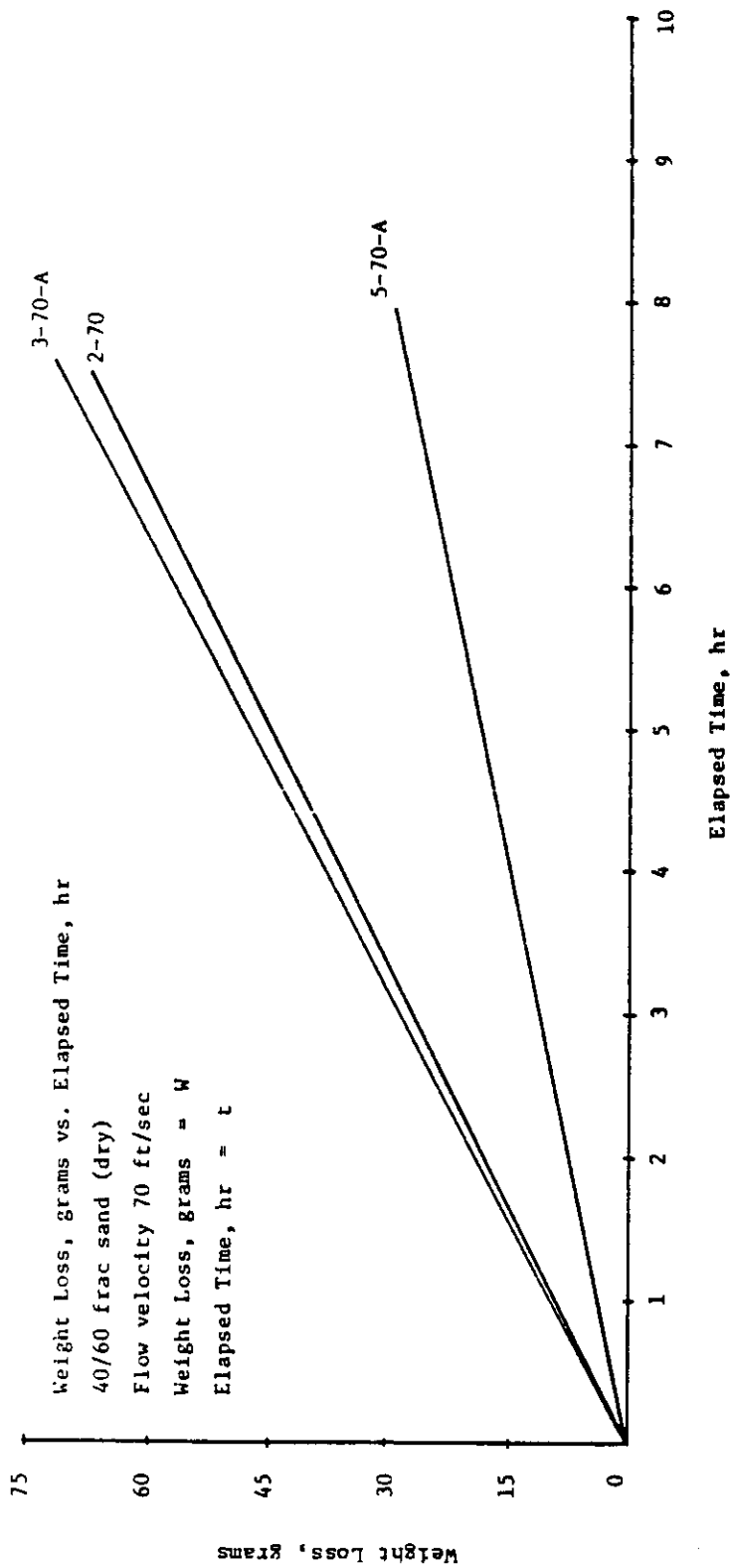


Figure 3.5 Wear Rate as a Function of Sand Flow Rate from Weiner and Tolle [9]

equation will primarily be of function of flow velocity and particle loading. The next category of service is corrosive flow streams without solids. The erosional velocity limits for this class of flows would contain terms related to corrosion such as CO<sub>2</sub> concentration, temperature, inhibitors, and two-phase flow parameters. The last category of flow is combined erosion and corrosion. Unlike the previous categories, no simplifications in an erosional velocity formulation would be available here since this must include all the parameters important for erosion and corrosion. The following sections discuss each of the different methods of pipe wear.

#### 4.1 Clean Service

No field data was obtained on erosion in two-phase flow lines that are free from corrosion and solids. While the occurrence of this type of flow is fairly limited, it would be applicable to a clean gas stream. For these "clean systems," a higher allowable erosion velocity is probably justified. Based on extensive survey of the liquid droplet erosion data, Deffenbaugh and Buckingham [10] suggested no velocity limit is necessary since erosion is not a problem until velocities are so high that practical pressure drop limitations are the limiting factor. Salama and Venkatesh [2] suggested setting the "C" value in the erosional velocity equation to 300. This recommendation is based on the high erosion thresholds reported for the onset of erosion due to liquid impacts.

It is felt that increasing the "C" value in the erosion velocity equation from 100 to the range of 200 to 300 is reasonable for clean services. The additional restraint of limiting the flow velocity to below 100 ft/sec is recommended to ensure the flow stays below the initiation point of liquid impact erosion. Since no field data or experimental data for flow in piping was available, the above recommendation should be applied cautiously until data is available to substantiate it.

#### 4.2 Erosion

While the erosion work done by Bourgoyne [8] was for high velocities and fairly high sand loading rates, it does provide carefully controlled experimental erosion data in pipe fittings. The experimental data shows the erosion in a fitting is directly proportional to the quantity of sand through the fitting and is independent of sand concentration (at high sand concentrations, interparticle interactions would start to reduce the specific wear factors). Based on Bourgoyne's work, an acceptable erosional velocity equation for erosion of pipe by sand can be developed.

Equations 3 and 4 above can be solved for the superficial velocity to obtain an equation for erosional velocity. To simplify the equation the following assumptions are made:

$$\frac{dh_w}{dt} = \text{acceptable wall erosion rate is } 4.02 \times 10^{-12} \text{ m/sec (5 MPY)}$$

- $\rho_s$  = pipe material density is steel, S.G. = 7.85
- $\rho_a$  = abrasive density is that of sand, S.G. = 2.65
- $\lambda_g$  or  $\lambda_l$  = for low concentration, volume fraction is approximately equal to 1.

The equation resulting from the above assumptions is:

$$V_e = K \sqrt{\frac{A}{q_a F_e}} \quad (\text{Eq. 5})$$

The information required to solve for the erosional velocity,  $V_e$  (m/sec) is the pipe cross-sectional area,  $A$  ( $m^2$ ), the volume flow of solids,  $q_a$  ( $m^3/\text{sec}$ ), and the specific erosion factor for a given fitting from Figure 3.2,  $F_e$  (Kg/Kg). The constant  $K$  in the above equation is equal to 0.000345. The above equation is for erosion only (no corrosion) in pipe fitting with fairly dilute sand in either gas or liquid flows. The assumption that 5 MPY of erosion is an acceptable erosion rate is included in the above equation.

While it would be nice to eliminate the need to know the sand production rate to predict erosion in piping, the nature of erosion is such that each particle passing through a fitting removes some material. Therefore, a prediction of erosion must include the quantity of sand flowing through the fitting.

Equation 5 above can be used to calculate a limiting or erosional velocity in sand producing wells. The calculated velocity is based on several assumptions and a limited data set. The following is a list of the assumptions and limitations that need to be considered prior to applying the above equation.

- Fitting wear is for erosion only. No corrosive effects were considered.
- Erosion data was taken only in 2" diameter pipe fittings so scaling effects to larger fittings are not available.
- The data was taken at very high velocity for application to production environments (the data was intended for diverter systems) and at very high erosion rates.
- Pressure effects were not included in the experimental data since all the data was taken at atmospheric pressure.
- The working fluids for the experiments were air for the gas testing and mud for the liquid testing.

- The abrasive in testing was #2 Blasting sand for all tests.
- The fitting temperature during testing was not regulated and is not incorporated into the wear equation. At the high wear rates experienced in testing, the fitting became "red hot".
- The data presented in Figure 3.3 seems to have a steeper slope than the line showing a slope of 2. The data for this fitting supports a slope closer to 3 (and, therefore, a dependence of wear rate with velocity cubed). If this is indeed the case for other fittings, the fitting erosion would fall off more steeply at lower velocities than predicted by the assumption of a slope of 2. The equation should, therefore, be conservative.

The above outlined limitations to the data indicate more testing would be useful in determining the applicability of Equation 5 for predicting an acceptable erosional velocity. Some of the issues that need to be addressed include: scaling effects with diameter, reduced velocities, pressure and real gas effects, pipe material, fitting installation effects (fully developed flow upstream of fitting versus flow from one fitting into another), temperature influence, and effect of abrasive size and geometry.

In order to independently test the erosional velocity equation developed above, it will be compared with the erosion work reported by Weiner and Tolle [9]. While identical tests were not performed in both test programs, the following describes comparable tests:

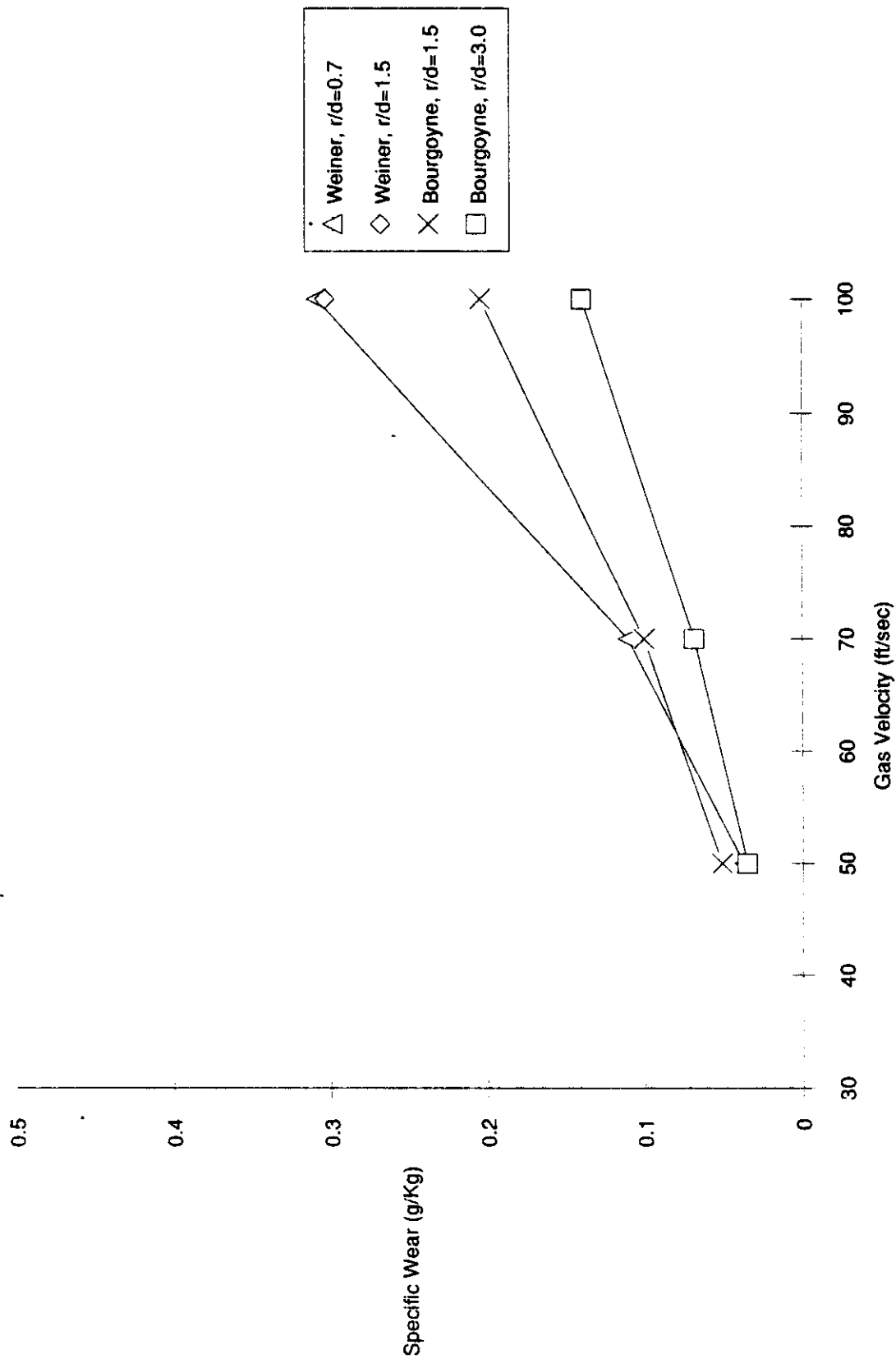
	Bourgoyne <u>Tests</u>	Weiner and <u>Tolle Tests</u>
Abrasive Material	Sand	Sand
Abrasive Size (mm)	0.6	0.3
Fitting Material	A216-WBC	Malleable Iron
Elbow Radius to Diameter Ratio	1.5-3.0	0.7-1.5
Fluid	Dry Air	Dry Air
Fluid Pressure	Atmospheric	Atmospheric

Figure 4.1 shows the Specific Wear plotted versus velocity for the above described tests. The specific wear values were calculated from Equation 5 above and from the data of Weiner and Tolle. The Specific Wear shown in Figure 4.1 is the ratio of the mass of material removed from the fitting to the mass of sand through the fitting. This should not be confused with the Specific Wear Factors,  $F_e$ , given in Figure 3.4 that relate wear to fitting geometry. While it is difficult to compare the data plotted in the figure because of the difference in fitting material (Weiner and Tolle did not specify the materials other than "field elbow" and "water elbow," they are assumed to be cast iron or malleable iron fittings), fitting geometry, and abrasive size, the following conclusions can be drawn:

- The magnitude of the specific wear factors shows general agreement.
- Weiner and Tolle's data shows a higher wear factor at 100 ft/sec. The reason is not obvious but may be attributed to the abrasive size, the fitting material, differences in fitting installation, or differences in the fittings internal flow path.
- Bourgoyne's data has less velocity dependence than Weiner and Tolle's data. This may be because the line shown for Weiner and Tolle is for a short radius elbow ( $r/d = 0.7$ ). Another possible reason for the different slope is, as described above, Bourgoyne's curve fit of the data (see Figure 3.3) seems to have a slope that is too flat to fit the data.

Even with the differences in the reported wear rates and test conditions, the plot in Figure 4.1 shows reasonable agreement between the specific wear factors. Based on this confirmation, Equation 5 can be used as a guide line to predict an erosional velocity where no other field operational experience exists. Before the equation is blindly applied to predicting erosion in piping, the following limitations in the data of Weiner and Tolle must be understood:

- All of the data was taken in 2" pipe.
- The wear rates were extremely high for application to the production environment.
- No corrosion was present.
- The data was for sand in dry air.
- The tests were all run at atmospheric pressure.
- The temperature of the fitting was not considered (the tests were performed at roughly room temperature, gas temperature was 120°F).



**Figure 4.1 Comparison of Specific Wear Rates Reported by Bourgoyne [8] and Weiner and Tolle [9] for 90° Elbows with the Given Radius to Diameter Ratios (r/d)**



- The lowest gas velocity tested was 50 ft/sec so extrapolation below this value is suspect.

The equation for erosional velocity developed here is based on the form of the wear equation being based on the velocity squared (Equation 5 has a square root term). Weiner and Tolle did not try to correlate their wear data based on the operating velocity, but a quick calculation based on the data in Figure 3.4 clearly shows that wear is proportional to velocity cubed. As noted above, Bourgoyne's data also seem to fit a wear is proportional to velocity cubed as well. While not enough data is presented by Bourgoyne to check this assumption, future work should investigate if a velocity squared or cubed term provides a better fit to the data.

### 4.3 Corrosion

The majority of the field data discussed in Section 2 included CO<sub>2</sub> or H<sub>2</sub>S in the product stream and are, therefore, considered corrosive. The data generally show that at velocities in excess of the erosional velocity (see Figure 2.1) wear is a problem. In addition, at velocities significantly below the erosional velocity, wear can be a problem due to accelerated corrosion (see Figures 2.10 and 2.11). Due to the wide variety of flow conditions and limited details on the flow stream contents, it is impossible to extract any recommendation for acceptable operating conditions in corrosive streams.

The above discussion confirms the recommendations in API RP 14E in that it states the erosional velocity should be reduced when corrosion is present. The API recommendation does not stipulate how to reduce the velocity and the field data reviewed here does not help in selecting any guidelines. Further work is needed in this area to determine the parameters of importance in controlling the corrosion rate. The field data does indicate that simply reducing the operating velocity does not arrest the corrosion for many different applications. The effects of temperature, PH, concentration of corrosion inducers, pipe material, water content, oil or condensate content, chloride concentration in the water, and velocity all interact and need to be investigated to provide guidelines for reducing corrosion to acceptable levels.

The data plotted in Figures 2.8 and 2.17 show that the present API erosional velocity criterion is probably of the correct form since it limits the operating velocity to below the onset of annular mist flow. Duncan [7] felt the transition to the annular mist flow regime was the cause of his accelerated wear problems due to either the inhibitor film or corrosion products were no longer able to provide protection to the pipe surface. Intuitively this makes sense since impact frequency is an important parameter in removing brittle material. With flow in the stratified or stratified-wave flow regimes, there would be no fluid impacts with the pipe walls. In the slug and annular mist

regimes, the impact severity and frequency increases dramatically. The data in Figures 2.8 and 2.17 clearly show this. Another way the flow regime can effect wear is that in annular mist flow, the pipe walls are repeatedly exposed to alternating gas phase and liquid phase.

#### **4.4 Erosion and Corrosion**

For flow streams that are corrosive and contain solids (sand), wear rates are usually very high due to the combined erosion and corrosion. The field data outlined in Table 2.2 shows only three entries with sand production reported. One reported a trace amount of sand and CO<sub>2</sub> with no H<sub>2</sub>S and had a wear rate of 5.6 MPY. The second report of sand production did not indicate if corrosion was a problem but still showed significant wear at 46 MPY. The third report of sand production was in addition to both CO<sub>2</sub> and H<sub>2</sub>S and an extremely high wear rate (1106 MPY) was reported. The two lower wear points had operating velocities below the erosional velocity, and the highest wear point had an operating velocity slightly above the erosional velocity limit.

As with wear due to corrosion only, wear in pipe lines with combined erosion and corrosion is a function of many different parameters in addition to flow velocity. Based on the limited field data, no recommendation for limiting the wear in the piping can be made and no determination of the most important parameters for developing an operational limit can be made.

### **5.0 RECOMMENDATIONS AND FUTURE WORK**

#### **5.1 Recommendations**

Based on the data reviewed during Phases I and II of this project, it is apparent the present form of the API erosional velocity equation is too simple to cover the wide range of conditions encountered in field piping. For this reason, it is recommended that the sizing criterion for multiphase flow lines be divided into four different groups based on the different wear mechanism. The reason for this is that each different wear mechanism will have a different set of controlling parameters that needs to be evaluated to limit pipe wear. The four different wear categories are:

- (1) Clean Service (no solids or corrosion),
- (2) Erosive Service (solids (sand) present in flow stream with no corrosion),
- (3) Corrosive Service (corrosion without solids),
- (4) Erosive and Corrosive Service (both solids and corrosive media present).

Recommended erosional velocity criteria for each of these categories cannot be made at this time. More work is required in the areas of Corrosive Service and Erosive and Corrosive Service. The required work is briefly outlined in the next section. While no recommendations for the form of the erosion velocity criteria in corrosive service is presently being made, it appears the present

format used in API RP 14E is a good start since it eliminates operation in the annular-mist regime. More work is required to verify this criteria limits wear in corrosive systems to an acceptable level. The velocity limit in corrosive service as it effects corrosion inhibitors also needs to be addressed. No recommendations for erosional velocity criteria in Erosive and Corrosive Service are presently being made. It is anticipated the operating criteria for this condition, will need to address the erosion of corrosion products by solids, and the acceleration of corrosion by increased surface exposure caused by erosion. The following outline presents the suggested sizing criteria.

## 2.5 Sizing Criteria for Gas/Liquid Two-Phase Lines

- a) **Velocity Limits.** Flow lines, production manifolds, process headers and other lines transporting gas and liquid in two-phase flow should be sized primarily on the basis of flow velocity. The limiting velocity is determined based on the fluid properties (corrosive or non-corrosive service) and if solids (sand) are present.
  - 1) **Clean Service.** Sand-free and corrosion-free service does not require any erosional velocity limitations. Pressure drop limitations will generally limit the velocity to below the threshold for erosion initiation. The velocity should be kept below 100 ft/sec to ensure the erosional threshold is not exceeded.
  - 2) **Erosive Service.** The flow velocity above which erosional damage may exceed an acceptable limit can be determined from the following equation:

$$V_e = K_s \frac{d}{\sqrt{Q_s}}$$

where:

- |       |   |  |
|-------|---|--|
| $V_e$ | = | fluid erosional velocity [ft/sec]              |
| $K_s$ | = | constant from the following table              |
| $d$   | = | pipe inside diameter [in]                      |
| $Q_s$ | = | solids (sand) flow rate [ft <sup>3</sup> /day] |

### K<sub>s</sub> Factors for Erosive Service (Adapted from Bourgoyne [8])

Fitting Type	Radius to Diameter Ratio	Material	K <sub>s</sub> Factor		
			Dry Gas Flow	Mist Flow	Liquid Flow
Elbow	1.5	ASTM 216-WBC	0.95	0.84	44.51
		ASTM A234-WPB	1.49	1.34	
	2.0	ASTM 216-WBC	1.00	0.91	44.51
		ASTM A234-WPB	1.58	1.46	
	2.5	ASTM 216-WBC	1.08	1.00	44.51
		ASTM A234-WPB	1.69	1.60	
	3.0	ASTM 216-WBC	1.15	1.10	37.62
		ASTM A234-WPB	1.82	1.73	
	3.5	ASTM 216-WBC	1.28	1.23	16.14
		ASTM A234-WPB	1.95	1.90	
	4.0	ASTM 216-WBC	1.48	1.41	14.07
		ASTM A234-WPB	2.10	2.01	
	4.5	ASTM 216-WBC	1.68	1.60	14.07
		ASTM A234-WPB	2.23	2.12	
	5.0	ASTM 216-WBC	1.99	1.90	14.07
		ASTM A234-WPB	2.38	2.28	
Plugged Tee	-	ASTM 216-WBC	8.73	5.56	20.75
		ASTM A234-WPB	12.85	7.04	14.07
Vortice Elbow		ASTM 216-WBC	15.94		26.60

- 3) Corrosive Service. To be determined.
- 4) Erosive and Corrosive Service. To be determined.

### 5.2 Future Work

In general, the data reviewed here shows that the present API RP 14E erosional velocity criteria does provide fairly reasonable pipe sizing guidelines. This can be seen in Figure 2.1 where the majority of data points that operate above the erosional velocity have pipe wear related problems. Other points on the same figure show when corrosion or solids are involved, wear can be a problem even below the erosional velocity. In addition, under other conditions, flow lines can

be operated above the erosional velocity without problems. This one figure clearly shows that several parameters, such as solids production or CO<sub>2</sub> concentration, need to be considered in setting operating guidelines.

There are many areas that could benefit from more work in predicting wear rates in multiphase flow lines. No "hard data" has been found for two-phase flow in non-corrosive service without solids in elbows, tees, and other fittings. A simple test at high velocity with "clean" fluids is needed to document no erosional velocity limit is needed in clean service. For multiphase flow with solids and no corrosion, the work of Bourgoyne [8] allows some estimate of fitting wear as outlined in Section 4.2. However, the data available in the open literature indicated that the root for sand flow may be higher than squared and as high as a cubed root. More data is needed to confirm the exact form of this equation. Other researchers [11] are presently working on erosive flow streams so future work in this project should be focused in other areas.

Wear in two-phase corrosive flow streams without solids is another area where laboratory quality data is required to develop a new criterion for limiting wear. Because there are so many variables involved in this type of flow stream, future work should focus on defining a velocity limit (or two-phase flow regime boundary) for a corrosion product film that is representative of "typical" field corrosion. Once the velocity criterion is defined for the "typical" corrosion product, a method that allows comparison of corrosion product parameters (adhesion, hardness, growth rate, . . .) with other types of corrosion products should be developed. Since corrosion inhibitors are typically used where corrosion is a problem, the effect of velocity on the corrosion inhibitor effectiveness should be determined. Another area requiring further work is erosion by solids in corrosive multiphase flow media. This type of flow problem is obviously very complicated and requires looking at many different flows, solids, and corrosive agent properties. Any experimental investigation of erosive/corrosive fluid streams would require focusing on trying to define a "worst case" boundary. This would mean selecting one corrosive fluid to work with while varying the liquid/gas/solid parameters to see how they effect the wear rates of a corrosive film.

## REFERENCES

1. American Petroleum Institute, "Recommended Practice for Design and Installation of Offshore Production Platform Piping Systems," API Recommended Practice 14E (RP 14E) Fourth Edition, April 15, 1984.
2. M. M. Salama and E. S. VenKatesh, "Evaluation of API RP 14E Erosional Velocity Limitations for Offshore Gas Wells," Paper No. OTC 4485, presented at the 15th Annual OTC in Houston, Texas May 2-5, 1983.
3. B. Craig, "Critical Velocity Examined for Effects of Erosion-Corrosion," Technology, Oil and Gas Journal, pp 99-100, May 27, 1985.
4. R. Heidersbach, "Velocity Limits for Erosion-Corrosion," Paper No. OTC 4974, presented at the 17th Annual OTC in Houston, Texas, May 6-9, 1985.
5. Raitel, Y. and Dukler, A. E., "A Model for Predicting Flow Regime Transitions in Horizontal and Near Horizontal Gas-Liquid Flow," AICHE J. 22, pp 47-55, 1976.
6. Mandhane, J. M., Gregory, G. A., and Aziz, K. A., "A Flow Pattern Map for Gas-Liquid Flow in Horizontal Pipes," Int. J. Multiphase Flow 1, pp 537-553, 1974.
7. R. N. Duncan, "Materials Performance in Khuff Gas Service," National Association of Corrosion Engineers, pp 45-53, July 1980.
8. Bourgoyne, A. T., "Experimental Study of Erosion in Diverter Systems Due to Sand Production," Paper #SPE/IADC #18716, SPE/IADC Drilling Conference, New Orleans, Louisiana, February 28-March 3, 1989.
9. Weiner, P. D. and Tolle, G. C., "Detection and Prevention of Sand Erosion of Production Equipment," Final Report on API OSAPR Project No. 2, Texas A&M Foundation, March 1976.
10. Deffenbaugh, D. M. and Buckingham, J. C., "A Study of the Erosional/Corrosional Velocity Criterion for Sizing Multiphase Flow Lines," Phase I Final Report, Minerals Management Service, U.S. Department of the Interior, March 1989.
11. Shadley, J. R., University of Tulsa, Private Communication, January 18, 1990.

